

Enhancing interlayer bond strength through diode laser assisted FDM process

Nurbol Sabyrov, bachelor's in engineering and technology

**Submitted in fulfilment of the requirements
for the degree of Master of Science
in Mechanical & Aerospace Engineering**



**School of Engineering and Digital Sciences
Department of Mechanical & Aerospace Engineering
Nazarbayev University**

**53 Kabanbay Batyr Avenue,
Nur-sultan, Kazakhstan, 010000**

**Supervisors: Dr. Md. Hazrat Ali
Co-supervisor Dr. Desmond Adair**

April, 2020

Acknowledgements

Firstly, I would like to offer my gratitude towards my supervisors Dr. Md. Hazrat Ali and Dr. Desmond Adair. Dr. Md. Hazrat Ali became my first mentor in the way of science. I am very thankful that professor believed in my abilities and skills. During the last years we wrote several manuscripts on different topics and making productive collaboration. Finally, under their supervision I am successfully finishing my Master program.

Secondly, I would like to show my gratitude to Ainur Satanova and Anuar Abilgazyev, the coordinator of laboratory and research assistance, which assisted me during experimental work and provided me with essential information about experimental process.

Abstract

The most widely spread and used 3D printing technology is Fused Deposition Modeling. The main reason for such usage due to its simplicity in manufacturing and low cost. The common problem of FDM is an anisotropic property of the extruded layer. An increasing number of new filament materials and their combination in the filling process decrease bonding strength between layers. Implementation of diode (450nm) laser with 5Watt power for localized heating of the pre-deposition layer proposed to overcome this problem. By controlling the power of the laser at the moment of printing, layer interface temperature reached for critical point, where the bonding diffusion process between layers increased for maximum level. Implementation of laser-assisted heating increased the ultimate tensile strength of PLA material to 9.67% at a laser power of 2.84Watt. However, the negative impact of heating on surface roughness also observed. The excessing laser power at a certain point leads to the formation of cracks and breaks on filament layers. This thesis described a control system used for adjusting laser power. The reported method is straightforward to use for other types of heating systems. Multi-directional heating system logic also was written in this work, where 3 diode lasers installed. The controller is capable of controlling many lasers at one time. In the case of printing objects with different filaments, it is also could be rewritten into controlling laser power deepened on filament type. The effect of the implementation of laser is analyzed from the energy and economic point of view. Even though energy consumption increases by 48% for energy cost, it is negligible. Regarding the financial aspect of implementation, the fixed price will rise by 53%, whereas the cost of electricity will be insignificant. Generally, the optimization of this method could bring more valuable benefits for the mechanical property of the FDM fabricated product.

Keywords: FDM, laser, interlayer diffusion, anisotropy

Table of Contents

ABSTRACT	Error! Bookmark not defined.
List of Abbreviations and Symbols	Error! Bookmark not defined.i
List of figures	Error! Bookmark not defined.ii
List of tables	Error! Bookmark not defined.x
CHAPTER 1-Introduction.....	10
1.1 Motivation.....	10
1.2 Objective of the research	11
CHAPTER 2-Literature Review	12
2.1 Effect of process parameter during the FDM process	12
2.2 Effect of temperature on bonding	Error! Bookmark not defined.
2.3 Pre-deposition heating methods.....	14
2.4 Conclusion remarks of literature review.....	19
CHAPTER 3-Design and Methodology.....	21
3.1 Methodology	21
3.2 Design of system.....	22
3.2.1 Hardware	22
3.2.2 Data transmission and control	24
3.3 Description of required components.....	25
3.3.1 The Laser Diode	25
3.3.2 Laser driver board	27
3.3.3 Arduino UNO	Error! Bookmark not defined.8
3.3.4 Connection of devices	Error! Bookmark not defined.8
3.4 Frame for laser attachment	29
CHAPTER 4- Experimental Design	33
4.1 Experimental setup	33
4.2 Laser control logic	36
4.3 Five Nozzle FDM printer.....	37
CHAPTER 5-Effects of Design	42
5.1 Effect of laser on Ultimate tensile strength	42
5.2 Effect of laser on surface roughness	45
5.3 Effect of laser implementation on energy consumption.....	47
5.4 Effect of laser implementation on the economic value.....	50
CHAPTER 6-Conclusion and Future Work.....	53
6.1 Conclusion	53
6.2 Future work.....	54
REFERENCES.....	55
APPENDIX A:Publication.....	59

List of Abbreviations & Symbols

FDM	Fused Deposition Modeling
AM	Additive Manufacturing
PLA	Polylactic Acid
ABS	Acrylonitrile Butadiene Styrene
\$	Dollar
t	Time [s]
W	Power [J/s]
E	Energy [J]
T	Temperature [°C]
I	Current [A]
V	Voltage [V]
A	Area [m ²]
P	Pressure [Pa]

List of figures

Fig.1.	Schematic of the experimental setup of the infrared lamp method	15
Fig.2.	Schematic of the forced air method	16
Fig.3.	The schematic view of the CO2 laser heating method	17
Fig.4.	The schematic view of 2-laser heating method	18
Fig.5.	Experimental apparatus schematic of solid state laser assistance.....	19
Fig.6.	Localized Heating System scheme	21
Fig.7.	a) Layer temperature changes during traditional FDM); b) Layer temperature21 change during heat-treatment	
Fig.8.	Angle, distance between laser beam fall and extrusion	23
Fig.9.	Top view of 3 diode lasers replacement for multi-directional heat treatment	23
Fig.10.	Process flow chart diagram	24
Fig.11.	5W-Laser diode	25
Fig.12.	Schematic view of a laser that includes current flow, beam and reflection angle	26
Fig.13.	TTL Driver (SW-LD73 V1.1).....	27
Fig.14.	Arduino Uno control.....	28
Fig.15.	Connection of devices.....	28
Fig.16.	The unsuccessful print of initial design of laser frame (design#1)	29
Fig.17.	Successful print initial design of laser frame (design#1).....	30
Fig.18.	3D view of frame for laser attachment	30
Fig.19.	Unsuccessful sample of the frame design#2.....	31
Fig.20.	Rotation part of the frame	31
Fig.21.	Laser attachment on printer nozzle part.....	32
Fig.22.	Tinius Olsen tensile tester.....	33
Fig.23.	Tensile sample dimension.....	34
Fig.24.	Tensile sample 3D view on Repetier Host software.....	35
Fig.25.	Motic AE2000MET microscope.....	35
Fig.26.	Laser power control logic	36
Fig.27.	Schematic view of 5-nozzle printer	37
Fig.28.	Extruder regulation section of the 5-nozzle printer	38
Fig.29.	Flow chart of the extrusion switch mechanism.....	39
Fig.30.	Printing of samples <i>a) before</i> and <i>b) after</i> adjustment.....	40
Fig.31.	“NU” –logo print.....	40
Fig.32.	Ultimate stress vs Laser power graph	43

Fig.33. Tensile test results of specimen 3.1 (PWM=100, 1.96W)	43
Fig.34. Break point of the specimen	45
Fig.35. The surface roughness of the specimen	46
Fig.36. The break formation during heating, “#0”without, “#2,4” with laser assistance	47
Fig.37. Printing time, number of layers and length of filament	48
Fig.38. Energy consumption of traditional and new method	50
Fig.39. Expenses for electricity of traditional and new method.....	51

List of tables

Table 1. Characteristics of Laser Diode	25
Table 2. Specification of Tinius Olsen tester	34
Table 3. Mechanical property of PLA.....	35
Table 4. Printing parameter of samples.....	36
Table 5. The actual cross-sectional dimensions	42
Table 6. Tensile test results	42
Table 7. Economical table value with price	51

CHAPTER 1-INTRODUCTION

1.1 Motivation

The Fused Deposition Modeling (FDM) is probably the most broadly utilized type of additive manufacturing technology in modeling and prototyping. The technology of FDM is similar to another type of 3D printing technology. The main difference from the traditional machining, which is based on material removal, in additive manufacturing technology material is to build layer by layer. The algorithm of the process begins from the 3D CAD model, designed on specialized software. Slicing of the object goes after converting this model into an “stl” type. Finally, 3D printing software prints products [1]. During FDM printing, the part building begins from bottom to top. Then thermoplastic filament is heated filament and extruded through the tiny hole and at the same time moved by controlled motors. The layer-by-layer final product is solidified. [2] FDM has several advantages, such as intricate geometry design, low noise and toxicity, lack of dust, and cheap maintenance cost. Although the Fused Deposition Modeling is a cost-effective process with simple technology, it could not fully replace conventional machining due to the following limitations: low mechanical strength, property anisotropy, dimensional inaccuracy, the surface roughness of printed parts. Moreover, for complex shapes support structures required, which should be removed further [1].

During the last decades, several aspects of the FDM process have been improved. Researches tried to enhance the quality of the part, general process improvement. In chemical laboratories, engineers attempt to create the new material type, with better properties and satisfactory characteristics. New ways of reinforcement of traditional filaments were created, fibers of bamboo and flax increased the modulus of PLA filament considerably between 91-230% [3]. Discovery of new applications of the Fused Deposition Process performed. The FDM can conquer pharmaceutical production, by solving the problem of drug degradation during extensive heating.

Nevertheless, dual printing technology opens the gates for further research [4]. In the area of the material property, essential studies focused on testing process parameters for specific material types. Investigation of process optimization concentrated on numerical simulations, recognizing the optimal extrusion path. Practical data of the tool-path generation approach showed its effectiveness [5] as well as material optimization method simulations

[6]. Object quality increasing, as surface finish, accuracy during extrusion also broadly studied.

Mechanical property is still the most important characteristics of the printed part. The high tensile strength and crystallinity make the final product firm. Experimental and mathematical model investigation performed by Pavan Kumar and Srinivasa Prakash explores the effect of filament bonding on the structural strength of the FDM printed objects. Ultimate tensile results indicate that inter-layer bonding is a key cause of strength [7]. Another paper dedicated to change of bond strength depending on deposition speed, layer height, platform, and nozzle temperature. They assert that higher temperatures of nozzle and platform, on par with fast printing speed and small layer height contribute good bonding. The authors explain that high interface temperature leads to an improvement in polymer diffusion [8]. Accordingly, research in this area has tremendous benefits in the way of enhancing the mechanical property of the FDM produced part. Moreover, the method of localized heating able to decrease the gap between layers in addition to strength [9]. Analyze existing systems that are proposed to heat surface temperature to rise interlayer bonding will be written in the literature part. The new method, based on controllable laser power will overcome the problem of these methods, as one-directional heating and took into account bonding between two different materials for a particular case of dual extrusion.

1.2 Objective of the research

The main goal of the research is to create a system for localized heating of the printing interface during the FDM process. The diode laser will be used as the main heat source. The controllable unit will be implemented to control laser power and laser power for maximum tensile strength will be found for various filaments. Another objective is designing applicable hardware and software systems. The number of sub-objectives is listed:

- Develop the new design of the laser-assisted FDM process, make it continent for most of FDM printer implementation; Create a system for multi-directional extrusion heating and solve the problem of other presented method in the literature review;
- Make an experimental investigation to recognize maximum laser power for best bonding; Programming of the control unit for laser power control;
- Find dependence between temperature and strength; Increasing structural strength, tensile strength by enhancing of bonding ;Analyze the surface roughness change of laser-assisted printed part;

CHAPTER 2- LITERATURE REVIEW

The tremendous potential of the FDM process becomes the main scope area of researches. Enhancing the overall process quality with a different approach was performed. Studies achieved a breakthrough in many branches of investigation. Overall, the effort of scientists could be divided into four groups of scope. They are: improving the printing process, developing new material and analyzing their property, increasing the quality of printed material. Among these topics, only a few branches relate to the presented thesis topic.

2.1 Effect of process parameter during the FDM process

The first important investigation direction is the process parameters. The process parameter has a considerable impact on the mechanical property of the fabricated piece. *Hongbin et al* [10] have investigated this effect on the bonding degree of the object during FDM. The outcome of the experiment showed the direct impact of parameters on tensile strength, which is determined by the bonding condition that is based on heat conversion between layers. The layer thickness, velocity of deposition, and infill rate are arranged by the level of impact [10]. Extruded part quality-analyzed and factors that influence to specimen property is found out in the study of *Tran et al.* [11]. *Jaya Christiyan et al.* performed tensile and flexural tests on ABS material based on ASTM D638, D760 standards [12] and short layer thickness and fabricating speed suggested obtaining maximum results.

However, *Hongbin Li et al.* [13] placed an air gap in the first place and defined layer thickness as a second key parameter during the tensile test. In the following study, the dimensional accuracy of Nylon, as well as tensile strength, is observed by changing process parameters as an orientation angle, shell, and layer thickness. *K. Basavaraj et al.* also characterizes layer thickness as the most significant parameter obtained by Taguchi array. [9] In a similar vein, *F. Górski et al.* [14] focused on the influence of process parameters on the dimensional accuracy of the model. Higher accuracy corresponds to high strength; however, cost increased also increased proportionally. Ultem 9085 was experimental material in the study of *A. W. Gebisa et al.* [15]. When the raster angle was equal to zero, it has the least effect, but in other values, it was the most significant on par with a counter number. *P. Vosynek et al.* [16] introduced the vital role of parameters on an object which has anisotropic structures. According to the experimental result, orientation during the process has high impact, and infill also defines the level of tensile strength. *Rajan Narang and Deepak*

Chhabra [17] did a similar experiment and get the following results: compressive strength of chemically processed object is better than without chemical treatment, raster angle has not reached the effect on surface finish. The mechanical property of polypropylene (PP) was selected as testing material by *L. Wang et al* [18]. FDM PP has weak tensile and structural strength characteristics compared to injection molded-PP. However, polypropylene molded at 250-degree exhibit lower change in mechanical property. *O. Mohamed et al.* [19] used analysis of variance (ANOVA) to measure which of the following parameters has a significant effect: layer thickness, raster angle, the width of extrusion road, and air gap. As the previous investigator, the authors highlight the significant impact of layer thickness and air gap. *Diana Popescu et al.* [20] wrote a review article related to the influence of process parameters on different specimen types (ABS, PLA, PEI, PEEK, PC, PA) during the FDM process. The paper includes the results of experimental and analytical data. The main established parameters are raster angle, layer width and orientation of the building. Filament bonding considered as defining in assessing of mechanical property printed part.

2.2 Effect of temperature on bonding

The bonding process of the layer directly depends on the temperature parameter. Different temperature conditions have a positive impact on this process. *Yan et al.* [21] did tensile experiments, by which they found out derived function and key parameters. The main conclusion of the study is that environment temperature has a greater impact than nozzle temperature. *Martin Spoerk et al.* [22] fulfilled experimental research on the impact of bed temperature on the adhesion of PLA and ABS fabricated samples. When the rate of temperature is just above the glass transition level, the surface tension between the heated bed and filament becomes lower. Moreover, the rise of bed temperature [23] increased and improved crystallinity, modulus, and strength of samples. In the mathematical and experimental experiments of *Taylor et al.* [7], they showed that tensile load was higher in parallel lay (extrusion direction), compared to perpendicular lay. In the study of *Naghieh et al.* [24] proved that post-heated scaffold and bulk exhibit higher elastic modulus on a curve. Keeping the specimen at a specific high temperature for not a long time leads to better material sticking between layers. In the investigation of *E.Fitzharris et al.* [25] tensile strength is increased from 52% to 80 and Young modulus rose from 57% up to 72% by utilizing heat-treatment. The same tensile enhancement pattern took place in the work of *Wonjin Jo et al.* [26] by thermal heating and at the paper of *Amir Reza Zekavat et al.* [27] during variation of fabrication temperature from 180 to 260 C. Hotter temperature caused better tensile results.

The article about the relationship between mechanical properties and crystallinity of Poly-ether-ether-ketone (PEEK) with nozzle, ambient, and heat treatment method was written by *C. Yang et al.* [28]. The crystallinity of material grew from 17% to 31% as the temperature of ambient changed within 25-200 Celsius. It is showed their close direct relationship. Nozzle process parameters considered as complicated. The furnace cooling method increased this parameter slightly, from 36% to 38%. *E. Kuznetsov et al.* [29] propose study on improving the strength of the FDM part by changing temperature-related parameters. Temperature factors considered as significant parameters defining the cohesion strength of the layer. One of the generalized factors was sublayer temperature. A small shift in temperature and melting characteristics indicate a structure change of PLA. [30]. *Q. Sun et al.* [31] explored the influence of processing conditions polymer bond quality. Experiment data showed that temperature has a big impact on the quality of the bond. This was based on the growth of the neck created between two adjacent layers. *T.J. Coogan et al.'s* [8] work has the following collisions: high temperature of the platform, nozzle temperature and fast fabricating speed on par with small layer height increase the bond strength of FDM part. As high, the interface temperature results in a greater filament diffusion chain. The next study research closely related to the proposed research. Implementation of a vacuum system on the FDM printing process minimized the cooling of ambient temperature, hence maintaining a warm field and lead to a better fusion of layers [32]. The investigation of *J. Yin et al.* [33] is based on the bonding process between layers during the extrusion of different materials, especially thermoplastic polyurethane (TPU) and acrylonitrile butadiene styrene (ABS). The authors explore inter-molecular diffusion between these two materials. Experimental evidence showed enhancement in bonding strength from 0.86 MPa to 1.66 MPa, via the change of building phase temperature between 30 and 68 Celsius. Intermolecular diffusion theory successfully applied for mathematical calculation of bonding strength.

2.3 Pre-deposition heating methods

The main purpose of this part is to familiarize with existed methods of heating the pre-deposition layer and find out the drawback of these designs. The mechanical anisotropy problem of printed parts restricts the usage area and potential of FDM. To address this problem the infrared preheating approach is proposed. The main method of which is the rising temperature of the printing area, before the new layer comes.

The experimental result indicates a 20% increase in bond strength of Acrylonitrile Butadiene Styrene (ABS) with a 20% of Carbon fiber. [34]. Schematic view with Infrared

lamps, Pyrometers, and extruder is shown in **figure.1**. To calculate the enhancement rate, a double cantilever beam test was performed. An experiment carried out in 3 different conditions. In the first and second conditions, 2 lamps with 500W were used, with different distances between heater and interface top, 8cm, and 2.5 cm, respectively. Moreover, at 1st condition after adjust printing speed of printer between 3.8 (cm/s) and 7.6 (cm/s). Regarding the 3rd condition, during this experiment, printer nozzle diameter was 7.62mm, whereas at other conditions diameter was 5.08mm. Most important, in this case, they used a single lamp with 1000W power, but the power intensity was kept at 81%. The black metal coverage was built to save heat and reduce disperse. The measurements of surface temperature were done by infrared pyrometers after precise calibration. The distance between the printing surface and the temperature sensor was 15cm, and 2 sensors made measurements. The surface temperature during the first condition did not reach the glass transition temperature level. However, an increase in printing speed was in direct ration with temperature increase. The second printing condition also was not successful. During the condtion#3, the authors obtained surface temperature, which is much more than the glass transition temperature value. If the required temperature was just above 100C, the implementation of an infrared lamp gave a temperature above 200C. Average fracture energy results taken according to 4-6 samples state illustrated significant increase during slow (3.8cm/s) and medium(5.1 cm/s) printing speed and almost no change in fastest (7.6cm/s) printing speed at condition#1. The same positive pattern was observed at condtion#2, but fracture energy at condtion#3 was low after heating, 6kJ/m² compared to 11kJ/m². The surface image with and without infrared heating indicates the influence of preheating. Based on these figures authors suggest keeping the surface temperature just a little bit above T(glass) transition temperature to decrease the spatial resolution and achieve good surface roughness.

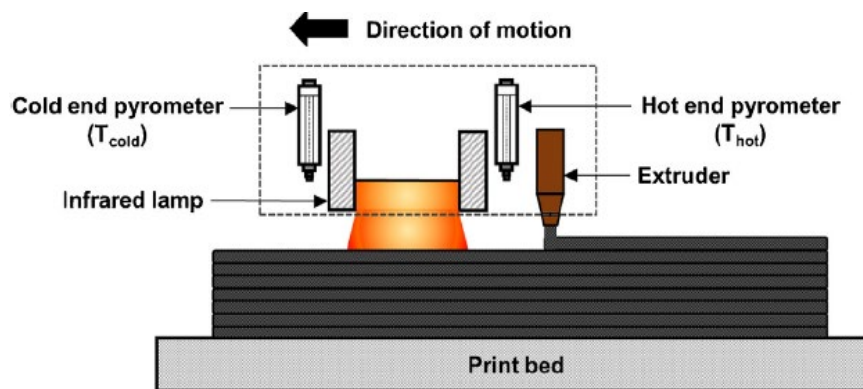


Fig.1. Schematic of the experimental setup of the infrared lamp method [34].

Despite the essential improvement, this design has some limitations. This method designed only for big area additive manufacturing. Increasing the temperature of a big interface is not effective, because the contact area between the new and previous layer is small, which is formed by thin extrusion thickness. There exists a waste of power for the heating excess area. The second restriction is the location of a heating system, which is launched on the top of the printer. This makes design inaccessible for common types of FDM printers.

Seth Collins Partain [35] presented a new method of pre-deposition layer heating based on forced air on his thesis. The welder is mounted on the printing device frame and air under pressure heats interface until the critical value. (see **figure.2**). Mathematical measurement on 45 samples performed to calculate dimensional accuracy. Chart result indicates that higher heating temperatures could decrease accuracy. The voltage factor was significant than the air pressure on dimensional accuracy. Initial design concern single copper tube was placed in front of the nozzle. This design had a negative effect as airstream blow melting filament that was just extruded and changed its extrusion path. The second design consisted of two tubes with a diameter of 0.254 cm. Although initial samples printed by this design were good, the copper tube several times undergoes heating and cooling process. The working temperature was not high compared to copper annealing temperature. However, many repetitions of the experiment made copper tubes soft. This problem, combined with continuous re-attachment of construction, shifted the alignment of air force position new the nozzle extrusion part The high degree of interlayer strength samples showed during fabrication under low pressure and high temperature. However, they had dimensional inaccuracy and low flexural strength.

Unfortunately, the author mentioned that this method did not show significant improvement in the FDM process because of the limitation of PVC welder and he faced difficulties with a lack of heat precision.

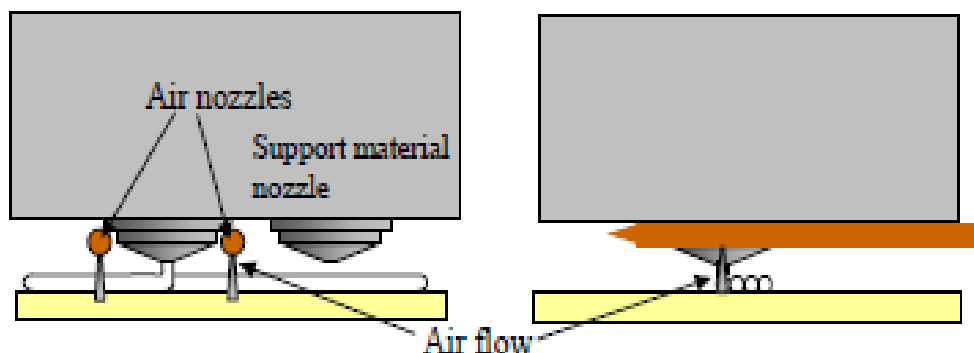


Fig.2. Schematic of the forced air method [35].

M. Luo et al. [36] highlight the PEEK material advantage and its tremendous potential. The issue of interlinear bonding during PEEK processing is improved by CO₂ laser. An essential increase in parameters of interlayer shear strength by 45% is observed, whereas crystallinity is changed almost twice. In order to see the impact of laser on shear strength authors vary laser power between 5%, 10%, 15% and 20% of total 40Watt. At the first stage with an infrared thermal imager, the authors find out the relationship between laser power and heating temperature. According to the graph interlayer bond point temperature, they are gradually increasing, while laser point temperature showed a significant increase. Because of excessive heating after a 15% intensity degradation period started. In the second stage, they highlighted the impact of laser assistance on crystallinity according to the DSC test, where frigid crystallization and melting points are apparent. The laser power increase directly enhances the crystallinity rate. These variables vary from 20% to 35%. The next stage related to bonding and temperature relationship. At laser power of 15% showed the highest increase in interfacial shear strength at 200C, where it was almost 18MPa, and the increase was 45%.

Further temperature heating gradually decreases the shear value. Another interesting observation is related to the air gap and the microstructure of the printed model. The SEM image taken under the heating 15% of laser power assistance and without laser showed little difference. For example, in the first case, it is clearly observed layer thickness, whereas after heating interface and layer separation could not be observed. The relationship between laser parameters and performance parameters is obtained, which means there could be used as a controllable system for obtaining specific interlayer shear strength value. The schematic view of the process is shown in **figure.3**. The disadvantage of this approach is a one-directional heating process out of 4. Only mirror 1 is fixed, while controlling the other 3 mirrors makes the system more complex. Another hindrance is 25% usage of a maximum 40W of CO₂ laser power, which leads to high energy consumption by laser. Consequently, the price of the printed part increases.

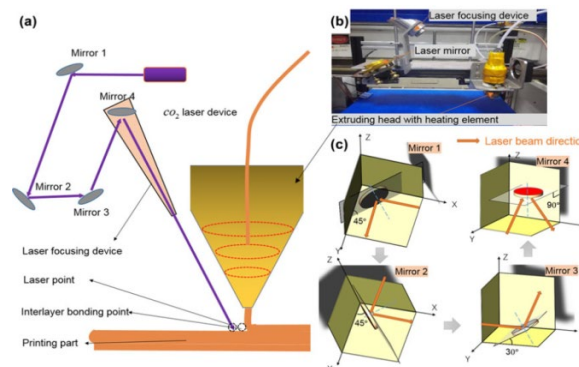


Fig.3. The schematic view of the CO₂ laser heating method [36].

Du Jun et al. implement infrared fiber lasers on the FDM process to produce large-sized thin-walled parts, as shown in **figure.4**. [37]. According to the tensile stress results, it was proven that a laser heating system could enhance tensile strength. Better strength could be obtained by stable laser power and printing speed, compared to pre and post-heating. 195% enhancement is observed in the tensile value of the fabricated part, compared to without laser assistance experiment. Graphical representation of speed and temperature dependence illustrates that low printing speed corresponds to high temperature. During conventional printing, the temperature gradually increases, whereas by application of laser some fluctuation could be observed. The viscosity graph shows almost similar results for both experimental conditions. The laser power changed between 0 and 2Watts, and the laser beam angle was 20 degrees, which has a diameter of 1 mm. The authors find out suitable speed ratio and layer thickness proportion, at 0.21mm of layer thickness width ratio was 75%. The obvious positive effect of laser could be seen online graph. At V20-x without laser heating, Tensile Strength stayed at 6MPa, where 1.75W it reached 15.5MPa value. A similar pattern shows other examples besides V10-x, where maximum tensile strength corresponds to 1.5W and a further increase in laser power decreased strength.

Regarding limitation, this technology is also created for a certain experiment and printer type. In order to carry out such an experiment, the FDM printer should be reassembled. However, this approach is considered to be the best from the list, because of fixed positions and laser type.

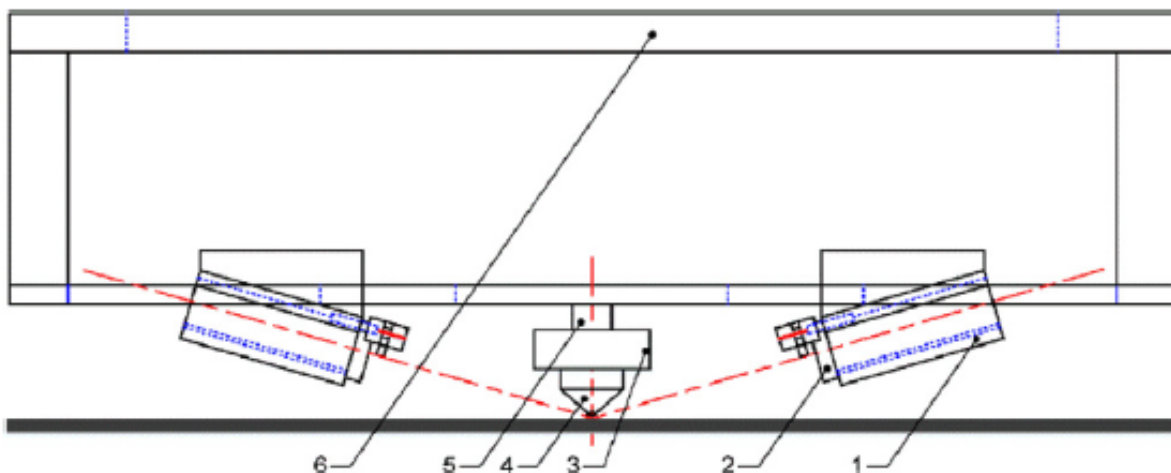


Fig.4. The schematic view of 2-laser heating method

K. Ravi et al. [38] presented a similar method of solving the problem of anisotropy property. The concept of the device which heats the region near the extrusion area before extruded material touches the layer. The design consists of 4 Au-coated reflective mirrors,

NIR coated Achromatic focusing lens and attenuator, as can be seen in **figure.5**. As a source of optical heater was used 802nm solid-state laser with a maximum power of 2W. The implementation of such an approach improves the strength of interlayer bonds by 50%. However, the excessive increase in laser power could cause defects between the hot and cold layers. Additionally, only one-directional heating is available. Another limitation is similar to other heating systems, and there is exist direction connection to the printing device.

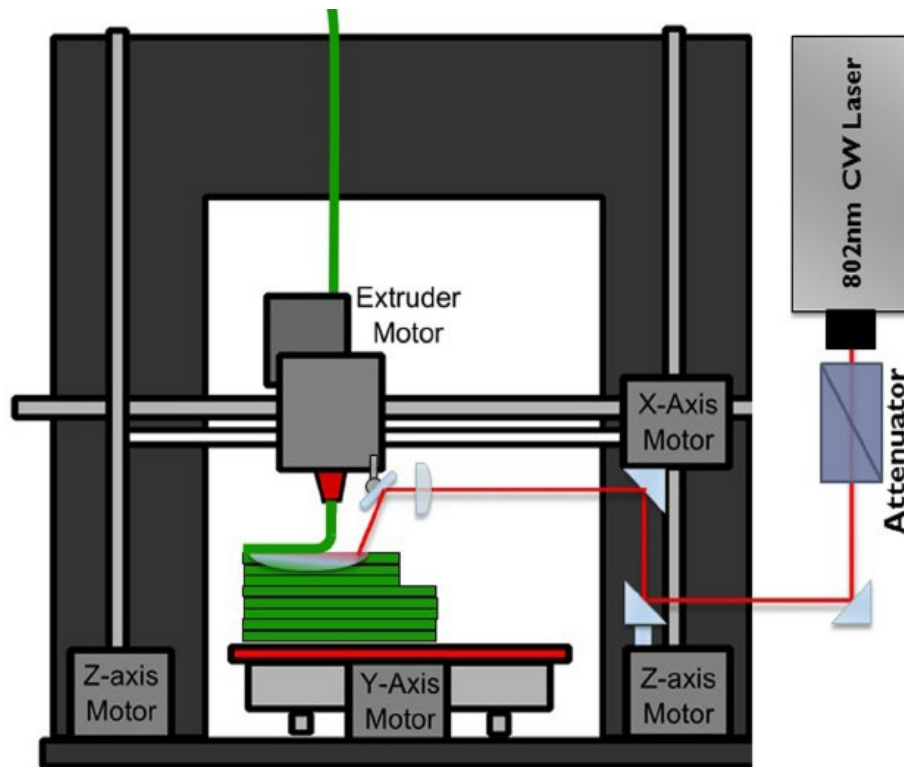


Fig.5. Experimental apparatus schematic of solid state laser assistance [38].

2.4 Conclusion remarks of literature review

From the primary literature review, the following conclusions are made. According to the studies of process parameters, they have almost the same pattern. Each process parameter has a different influence on the property of the printed part. The best process parameter for one material property negatively affects another material feature. In case when the high surface roughness is required, the temperature of the extruder should be low, but it reduces the durability of the printed object. Decreasing the thickness of the layer is proposed to achieve a high bonding degree, increases printing time.

Heat treatment during the FDM process could increase important parameters of the printed object. Tensile strength, Young modulus, and crystallinity of the extruded part increased considerably. Additionally, cohesion strength and bonding between layers enhanced by following conditions: furnace temperature, ambient temperature, nozzle, and building

stage temperature. The key to the improvement of the quality of the FDM printed part becomes temperature.

Analyze these 5 pre-deposition heating approaches again highlighted the essential impact of heat treatment. Considerably increase in bonding value was obtained by a different method. Each of these experiments and design has drawbacks. Different methods focused on heating of printing material surface before the following of a new layer. This is the main method of increasing the interlayer bond strength.

CHAPTER 3-DESIGN AND METHODOLOGY

3.1 Methodology

The key method of increasing structural strength, the tensile strength of a 3D printed object is a strong bonding between layers. The bonding process happens at a molecular level. The rise of temperature stimulates the diffusion process. The heating operation is carried out by laser (see **figure.6.**). By heating along the filament fall path, laser warms the last layer to glass transition temperature to get high bonding.

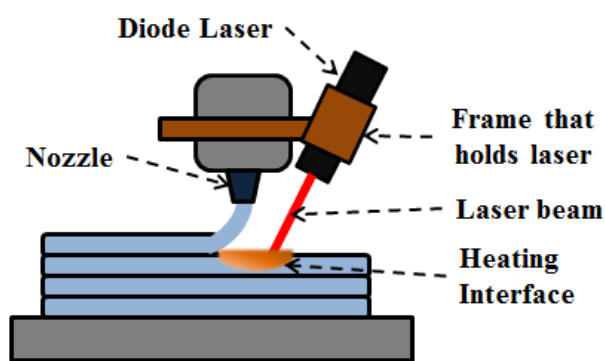
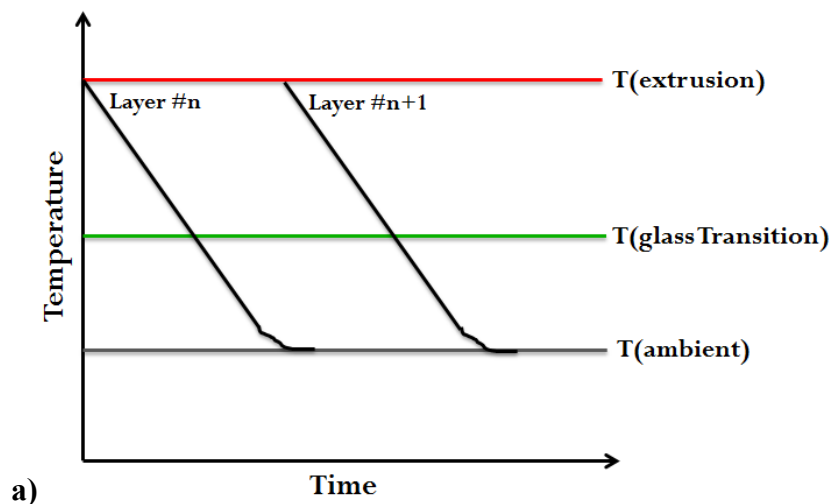


Fig.6. Localized Heating System scheme

The diagram of the layer temperature change in the conventional FDM process is illustrated in **figure.7 (a)**. In traditional printing “layer n” temperature drops from melting point to environmental. At the moment of coming new, the old layer already cooled down. Consequently, binding between layers diminishes. The implementation of laser heating solves this issue. Just before extrusion of “layer n+1”, “layer n” is started warming until the glass transition temperature (see **fig.7 (b).**)



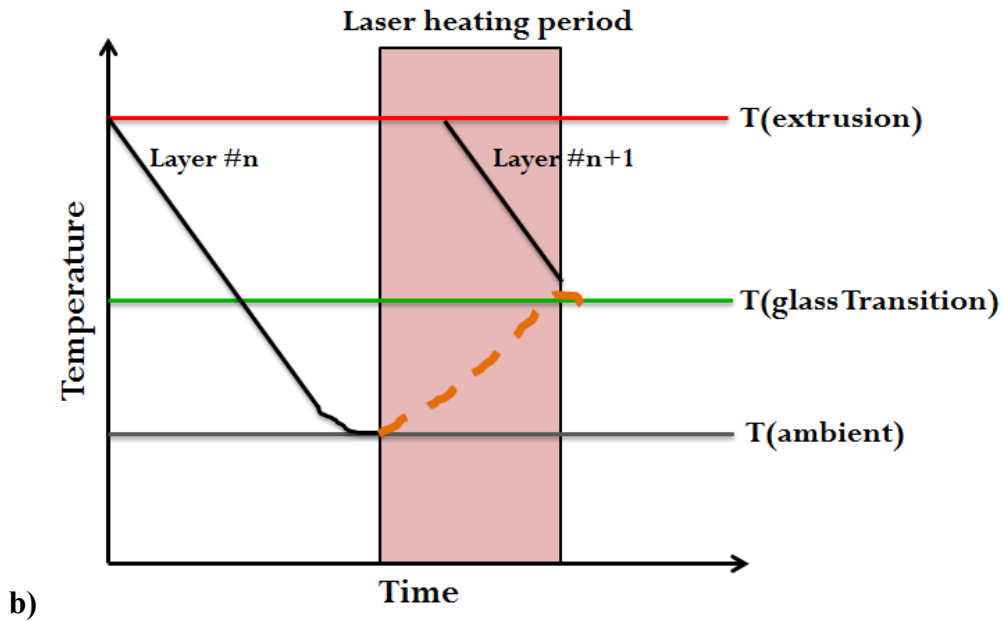


Fig.7. a) Layer temperature changes during traditional FDM); b) Layer temperature change during heat-treatment

3.2 Design of system

The laser pre-heating system consists of two parts. The *first one* is the hardware equipment that provides laser beam control. To create a system that could be mounted in any FDM 3DP, it should be easily removable on the printing machine. In the proposed system hardware will be directly mounted on the nozzle of the printer, the lightweight of diode laser and frame allows keeping the same accuracy and speed because the new system has low pressure on the nozzle part.

The *second part* of the system is data transmission between the 3D printer and laser control system. It is the logic of the system, which will control the power of the laser according to the temperature sensor and filament type received from the printer software.

3.2.1 Hardware

The hardware of the system is intended to perform the heating operation. It consists of the laser diode, temperature sensor, and controller. The laser is attached to the nozzle of the printer. **Figure 6** shown laser, which is a little bit rotated along its axis. This design helps to laser beam reach to the printing interface without any mirror. The distance between nozzle printing point and laser beam hit a point around 3mm. This distance should be enough for the laser beam to heat. However, this distance could become longer if the power of the laser is low. During the time, when the nozzle passes this distance, the laser beam should quickly

increase interface temperature. **Figure 8** illustrated the α -angle between extrusion and laser beam fall point.

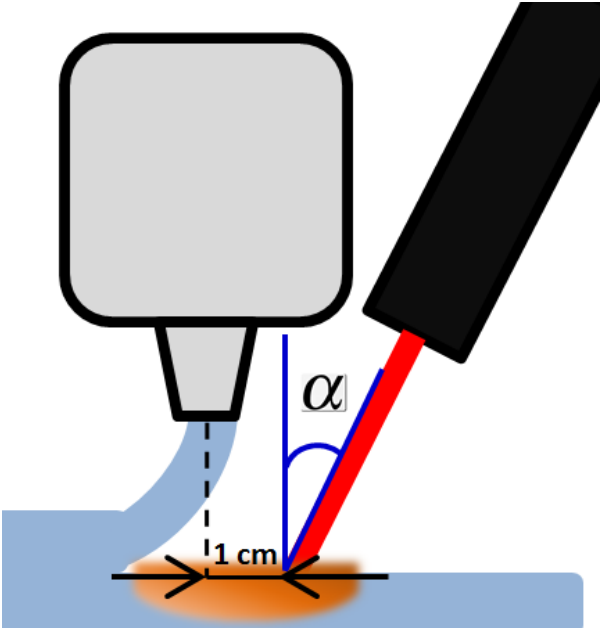


Fig.8. Angle, distance between laser beam fall and extrusion

In the case of the multi-directional movement of the nozzle, the heating system could be extended. For this goal, 3 diode lasers will be replaced around the nozzle and heated to each side. The angle between two subsequent laser diodes is 120 degrees. In the case of the extrusion path, which will be located between two close lasers, both of them will be turned on, whereas another is turned off. Replacement of these lasers will allow the whole cover interface of extrusion. Distance is a 1 cm radius, which is close enough to intersect to two laser heating regions together.

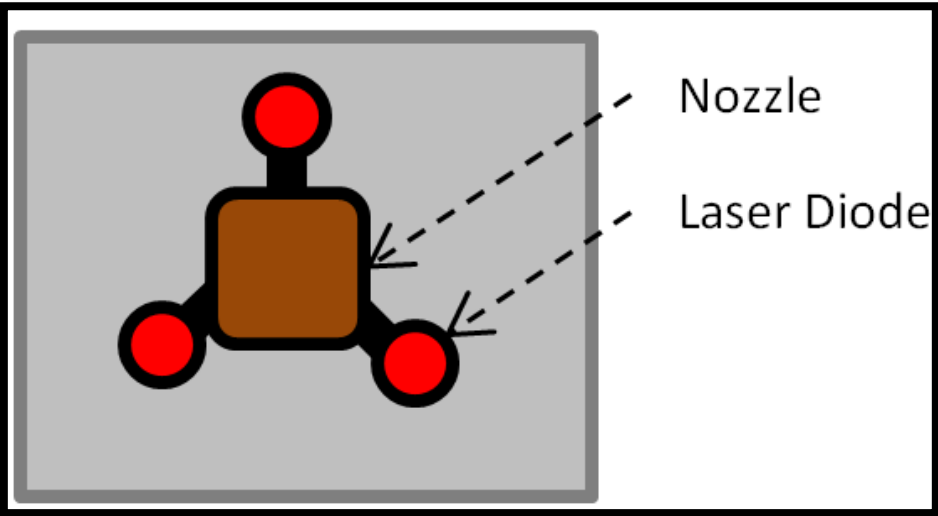


Fig.9. Top view of 3 diode lasers replacement for multi-directional heat treatment

3.2.2 Data transmission and control

A controller is responsible for data transmission and control. The signal from the temperature sensor sends information about the current state of the interface. Then the controller calculates and sends a signal to diode laser, to turn on or turn off. The main advantage of this system is the following, a controller connected with the main software of the 3D printer, where it takes information about the material type. Depending on the filament type, the controller changes the power of the laser. Hence, for each material laser will heat interface temperature until glass transition level to achieve peak diffusion. Additionally, in the case of multi-directional extrusion, the controller will change the power of a specific laser. For example, if nozzle extruding in a forward direction, laser 1 turns on, if backward direction, it activates another laser. For the diagonal movement, two closest lasers will be operating. General logic and architecture of data transmission and control are illustrated in figure 10.

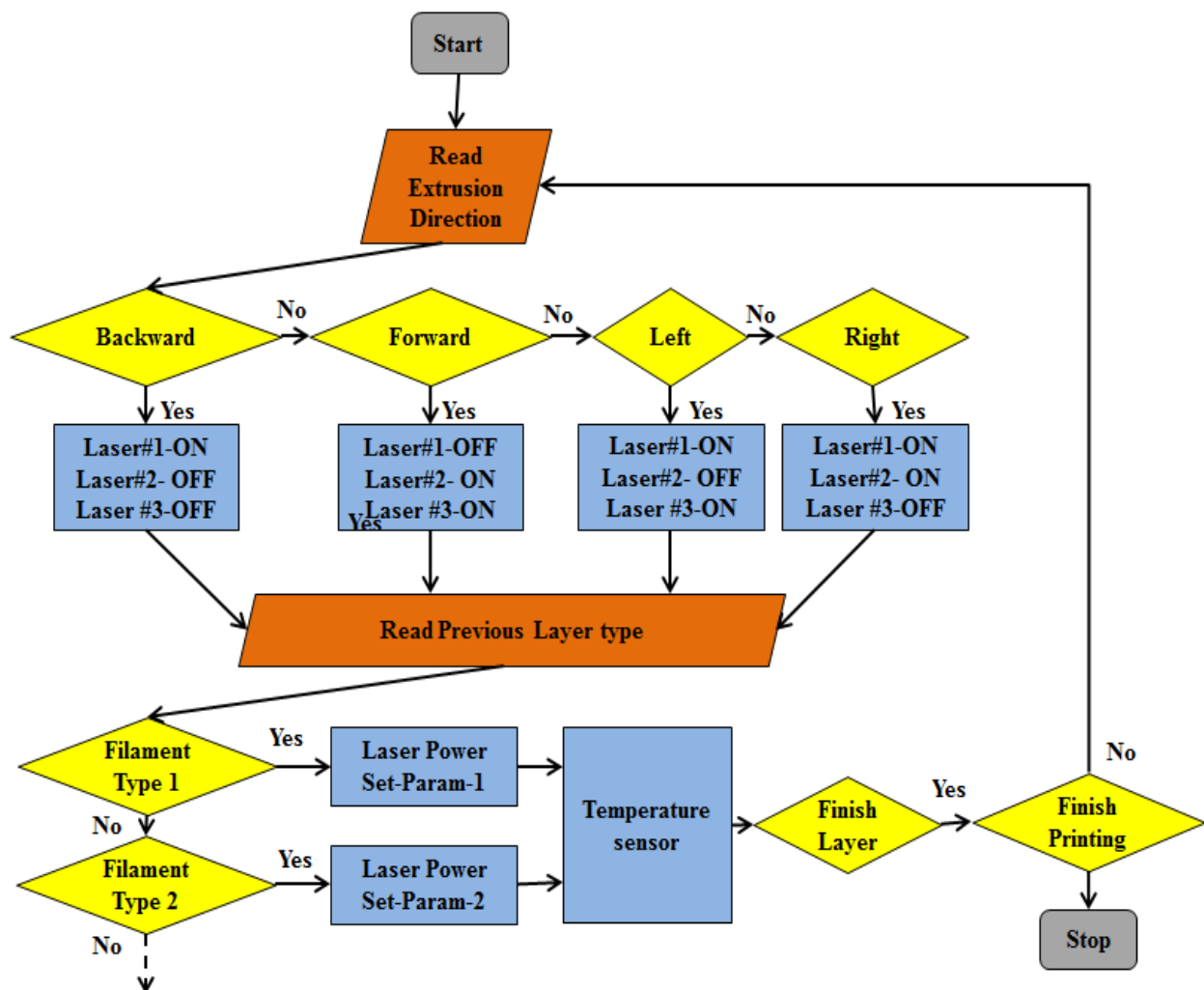


Fig.10. Process flow chart diagram

3.3 Description of required components

3.3.1 The Laser Diode

The main component of the design is a laser diode. **Figure 11** illustrates the laser diode appearance. The main characteristics of the 5W power laser listed in *table 1*. Generally, the diode laser working principle and construction are similar to the light-emitting diode (LED). This semiconductor apparatus emits light through the way of optical amplification, which is generated by electromagnetic radiation. Hence, it converts electrical energy to light. The common usage of the laser diode takes place in CD-ROM players. The laser diode has simple circuitry and could emit power from mill watts to hundreds. The compact size and current modulation system, which allows high-speed data communication, counted as an important advantage of a laser diode.



Fig.11. 5W-Laser diode

Table1. Characteristics of Laser Diode

Parameter	Data
Laser Wavelength	450 nm (blue-ray color)
Output Power	15W
Work Voltage	12V
Work Current	5A
Focal length	16mm
Driving Mode	Constant ACC
Modulation	TTL
Dimensions	85mm*33mm*33mm

The diode laser has several advantages compared to its competitor as solid-state laser or CO₂ lasers. The lightweight that comes from a small size, the low power consumption makes it a cost-effective device. Such kind of properties made diode laser usage area very huge. It is commonly used in electronics, medicine, and communication. [39]

The threshold current, slope, and temperature characteristics are the main characteristics on which depend its function. The slope of L-I characteristics defines the efficiency of the diode laser. Even the best available diode laser in the market could reproduce 50% of input current to laser light. [39] Diode laser is very sensitive to temperature change. However, each laser has its thermal stability value, which represents the threshold value of temperature where it works effectively. The high sustainability value of laser means low effect by the temperature of the environment. [39]

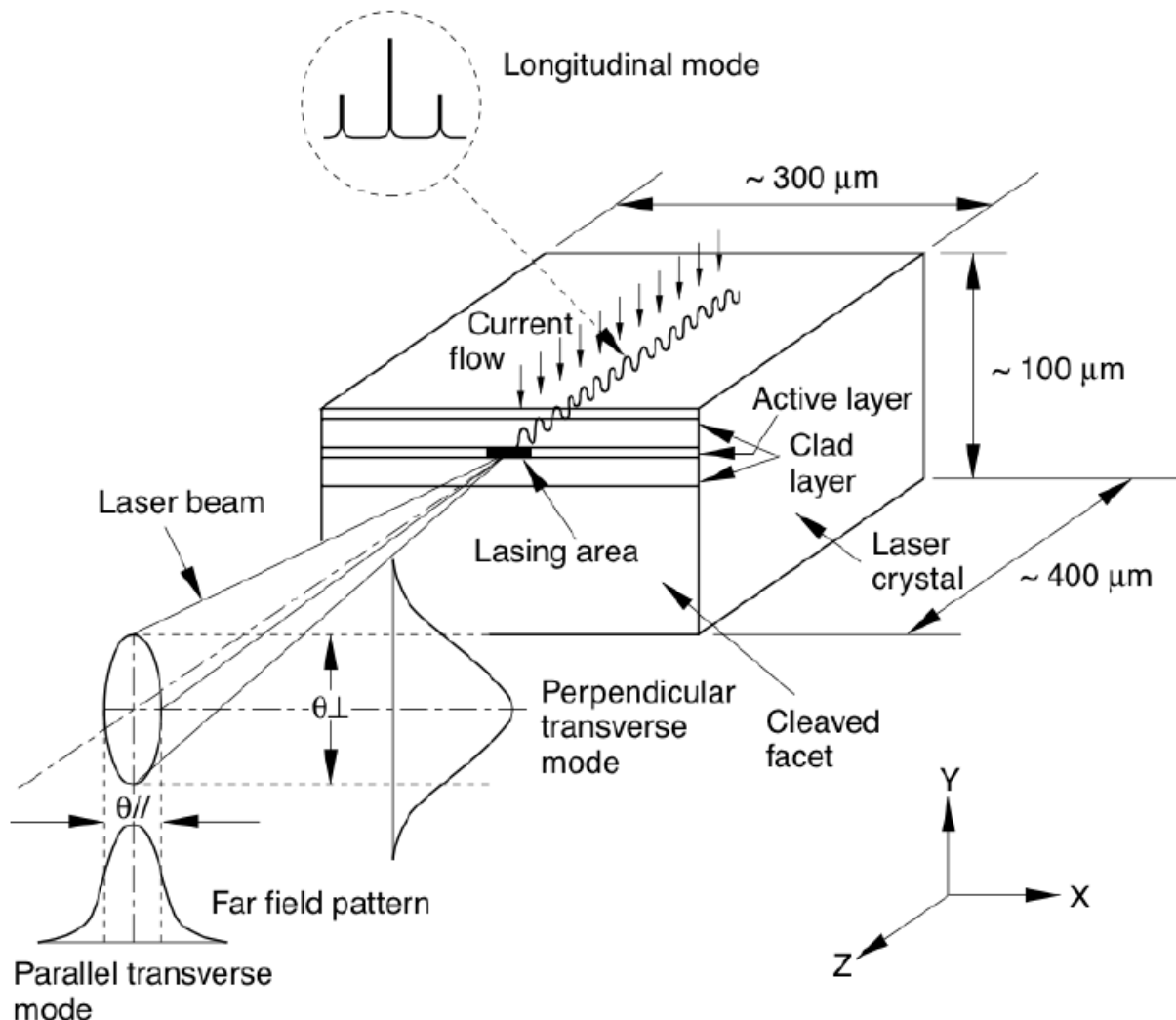


Fig.12. Schematic view of a diode laser that includes current flow, beam and reflection angle [39]

Another feature of the diode laser is that photons used for stimulating emission by interaction with electrons, to liberate extra photons with similar frequency, phase, and travel direction. The laser generation process requires a certain condition. The rate of emission must be more than the amount of absorption of photons. Hence, amplification happens as well as population transposition. Output power produced by a diode laser could not remain stable and due to external noise, it fluctuates. Nevertheless, output fluctuation power value is stable concerning the total output value. [40]

Figure 12 shows a detailed view of a traditional diode laser with a double hetero structure. The cladding sections have semiconductors material of n and p-type. In the middle of the cladding, the section placed an active layer, and in this layer, laser light is produced. The shape of the laser beam is divergent and has an elliptical shape, and this occurred due to the lasing area nature. Naturally, it has a rectangular area, and because of diffraction, it changes its shape to elliptical that has a small height on the “y”-axis. Consequently, it creates big perpendicular transverse mode related to small mode. [39]

The lasing pick value directly depends on the threshold current, which allows charge processing. This current, on the other hand, depends on the temperature value of the device. [41]

3.3.2 Laser driver board

The laser power control is accomplished via the TTL (Time To Live) driver board. The version of SW-LD73 has Input ports which are supplied by 12V voltage source. Moreover, the driver contains a TTL port, where they could be sent PWM (Pulse Width Modulation) signals. To adjust laser power to a lower degree, it is possible to use a switch on the top of the driver. Near the voltage source, it has an additional PWM port for Arduino. On the other side of the port replaced output ports. The driver could power laser supply and fan port, both of them (see **Figure.13**).



Fig.13. TTL Driver (SW-LD73 V1.1)

3.3.3 Arduino UNO

To adjust laser power and calculate specific laser power for certain material Arduino Uno used as a controller. The operating voltage of the controller is 5V. To supply controller laptop USB port could be utilized. It has 14 digital port, 6 of them provide PWM signal type. Additionally, the controller has 6 analog pins. The clock speed for data transmission is 16MHz. The USB connection port allows the user to connect it to the computer and download the program (see figure.14).



Fig.14. Arduino Uno control

3.3.4 Connection of devices

The laser driver shield has already ported for laser positive and negative wires. The laser could be supplied from an external 12V or this shield.

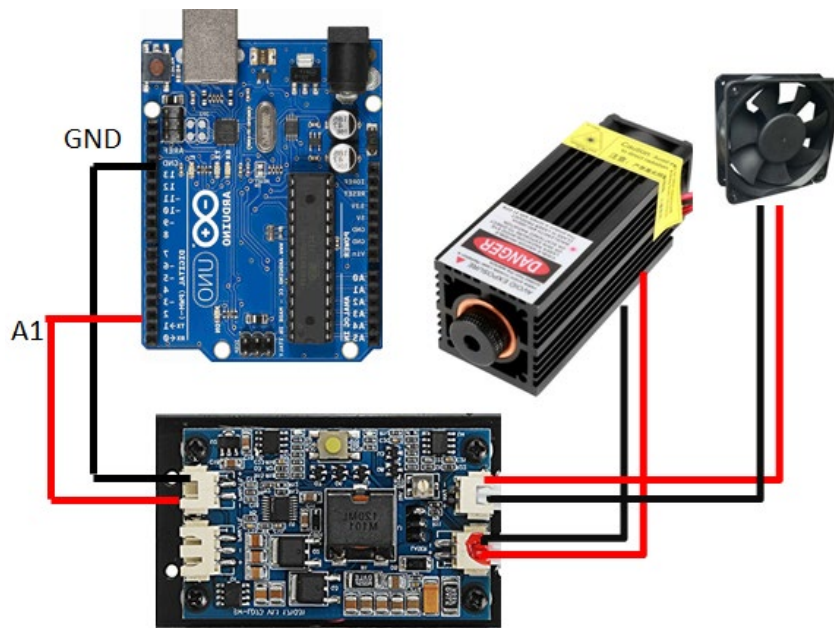


Fig.15. Connection of devices

The fan used for cooling of laser replaced behind the laser, it has 2 wires (+-) which are also connected to TTL driver. Arduino GND is connected to TTL(-), whereas TTL(+) is connected to the A1 pin, which supports the PWM signal. The power of the laser is controlled via analog (A1) pin. This port has an analog output of 5V, by doing mapping from 0-255 (8bit), which is equal to 0-5V, it is possible to change the brightest of the laser diode. For example, the 128 sent from Arduino transform to 2.5V of the output voltage at the A1 pin. Therefore, operating laser power becomes 2.5W. The general apparatus connection is represented in **figure 15**.

3.4 Frame for laser attachment

To attach the diode laser on the FDM printer nozzle part, a special frame was designed. The design of the laser frame modified during the printing process. Initial design printed unsuccessfully due to shifting during printing. **Figure 15** illustrated the brake that was caused by poor bonding. Another successful try of printing design #1 (see **figure 16**.) showed its disadvantages. After the implementation of design#, 1 sample printing was launched, but the laser was turned off. During the printing, the process frame started to vibrate on the “y” position, where the extrusion path changed its speed and position very fast. The weight of the laser was too high for the frame to hold it in a stable position.

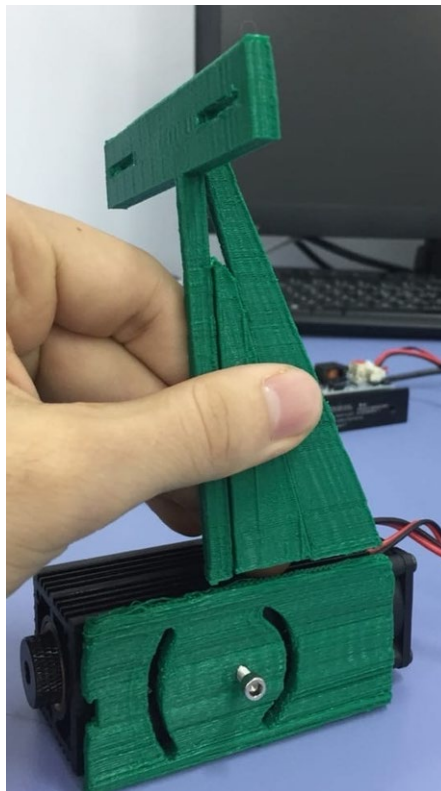


Fig.16. The unsuccessful print initial design of laser frame (design#1)

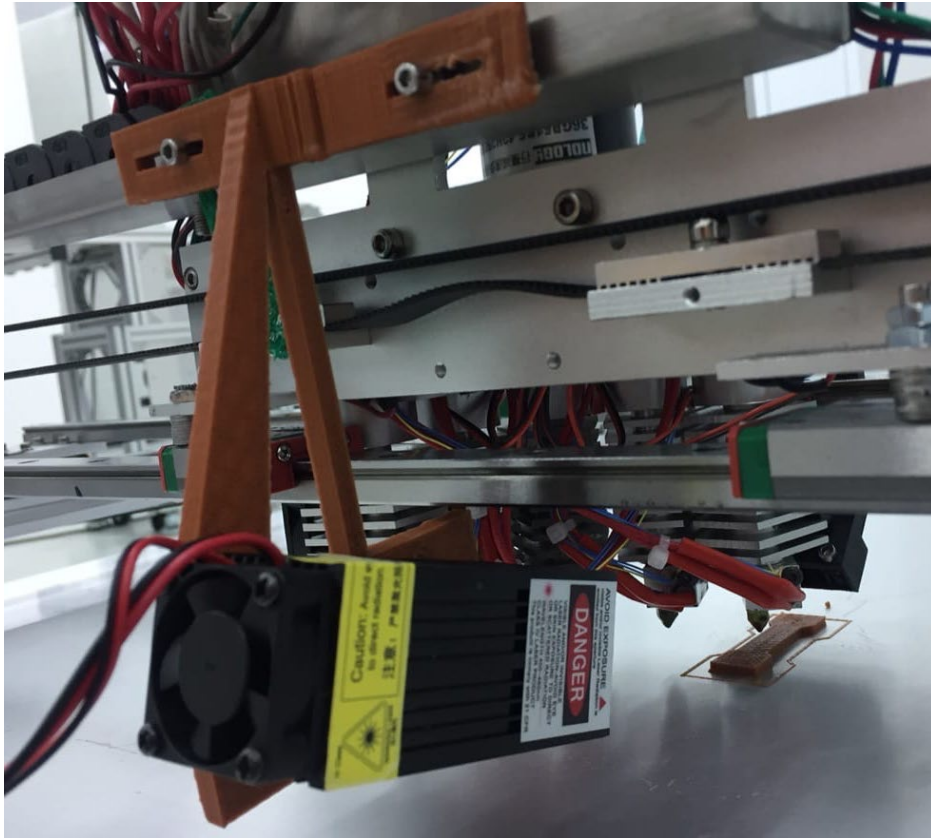


Fig.17. Successful print initial design of laser frame (design#1)

To reduce vibration, design#1 was modified. The main reason for frame vibration was the thickness of the frame wall. For this purpose, the wall thickness was increased up to 8mm. Figure 17 showing a 3D view of frame design#2 on SolidWorks software.

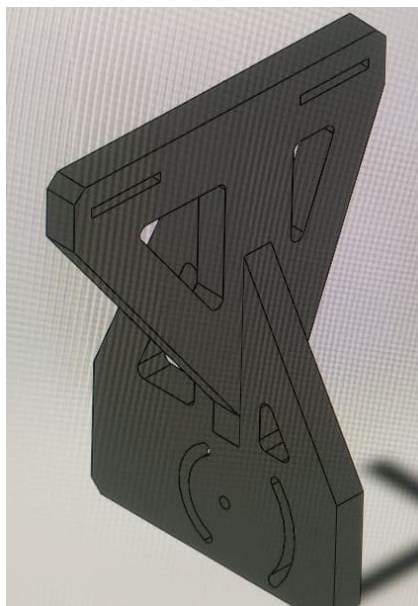


Fig.18. 3D view of frame for laser attachment

Additional supports on both “y” and “x” direction were designed. This kind of bracket allows eliminating vibration because it fully distributed along with the frame. The initial printing sample was unsuccessful, which could be seen in **figure 18** and caused by bad bonding and change of the extrusion path of the printer.



Fig.19 Unsuccessful sample of the frame design#2.

The design model of the frame enables to rotate laser frame, which allows the control laser beam angle, which is shown in **figure 19**. This is accomplished by changing 2 bolts of a laser. The central bolt is fixed, whereas the other 2 could change position (see **figure.20**). Additionally, this model is attached to the nozzle part of FDM by 2 bolts. Special space was made for these holes, a distance of 20mm. Along with this distance, the whole frame position along X-axis could be adjusted.



Fig.20. Rotation part of the frame

The final model of the frame is shown in **figure 21**. This design allows for eliminating vibration during the printing process.

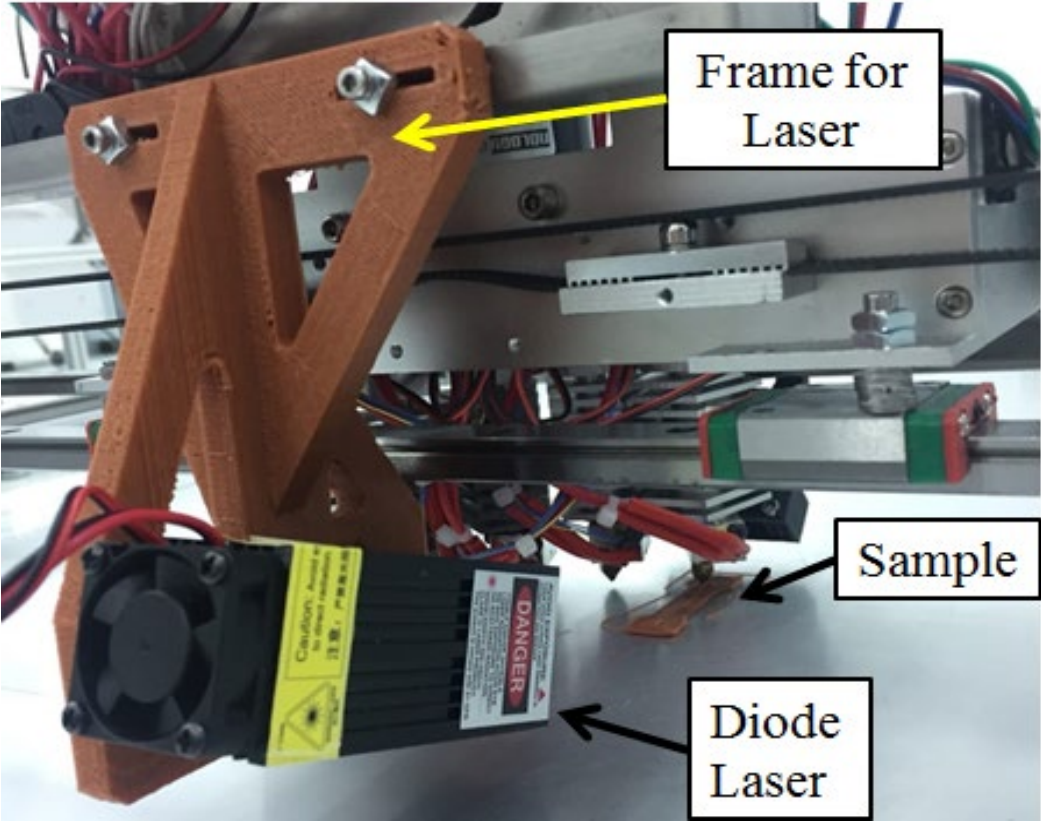


Fig.21.Laser attachment on printer nozzle part

CHAPTER 4 – EXPERIMENTAL DESIGN

4.1 Experimental setup

Investigating the positive effect of the laser-assisted FDM process requires an experimental test. Rising of interface temperature increases the bonding of layers during the printing process, which means printed objects become stronger structural. Hence, the tensile machine used to analyze tensile properties specimens. Tensile stress performs the task during which the ultimate tensile and yield strength could be observed. During this experimental work, Tinius Olsen tensile will be used, which is shown in **figure 22** with characteristics described in *table 2*.



Fig.22. Tinius Olsen tensile tester

Table 2. Specification of Tinius Olsen tester

Parameter	Data
Force resolutions during measurements	1/320000 of load cell capacity
Accuracy of Force	±0.5% of the nominal load in range 2 -100% of load cell
The sampling rate of Force	200 Hz
Extensional Resolution	0.001 mm of the complete cross travel
Accuracy of Speed	±0.05% of the set velocity
Working environment	Operating temperatures range from 0 to 38°C

The sample dimension is different from the standard dimension of tensile test protocols. In order to measure the effect of heating, the tensile sample size changed. Standard height increased to 5mm, and this gives a sufficient number of layers. Based on the size of the tensile machine, the width dimension set to 15mm. Internal width is equal to 9mm that gives enough lines of extrusion path. The complete size of the specimen is shown in **figure 23**.

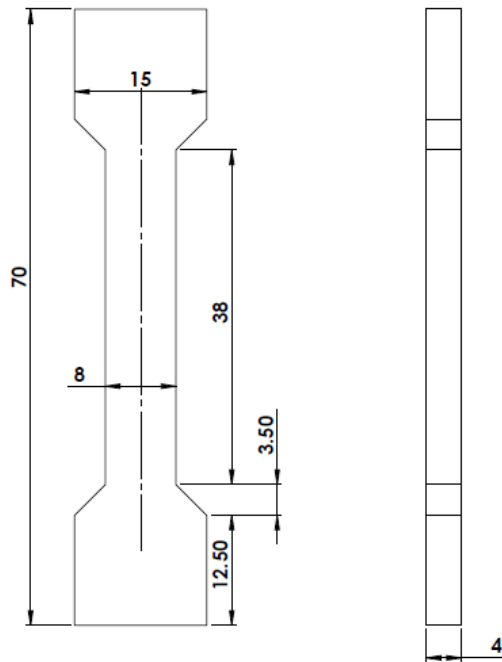


Fig.23. Tensile sample dimension

Slicing process carried out on Repetier Host software, a special program for the FDM printer. After downloading the STL (stereolithography) format file in this software, it automatically makes slicing. The building edge is along Z-axis (height). Printing and heating along long Y-direction give us a high bond between layers. The 3D view of the tensile specimen is drawn in **figure 24**.

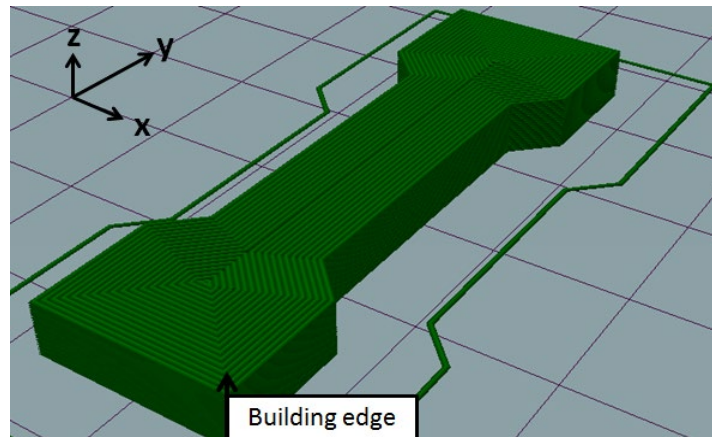


Fig.24. Tensile sample 3D view on Repetier Host software

The PLA (Polylactic acid) material is chosen as a printing material. PLA is produced from organic material. Compared to ABS (Acrylonitrile Butadiene Styrene), during the printing process, it is more likely liquid than ABS. Hence, the printed model is more detailed. The mechanical property of PLA described in *table 3*.

Table 3. Mechanical property of PLA

Parameter	Data
Flexural Modulus	4 GPa
Density	1.23 g/cm ³
Melting Point	180
Glass Transition Temperature	60C

To observe the effect of laser heating on the surface of the printed part, Motic AE2000MET microscope was used. The zoom of 50 allowed us to view the influence of heating on a surface closely. The device has a direct connection with the computer, where further manipulations with images could be done. The software of apparatus has measuring tools, by which the distance of hole and gap could be measured.



Fig.25. Motic AE2000MET microscope

Table 4. Printing parameter of samples

Parameter	Data
Printing speed	35mm/s
Extrusion temperature	208-210°C
Bed temperature	51°C
Diameter of Nozzle	0.4mm
Retraction speed	30mm/s
Side thickness	8mm
Environment Temperature	20°C
Filament	PLA(chocolate color)

On *table 4* listed the printing parameters of samples. The most interesting point is the printing speed. The initial tests were performed to establish the comfort speed of the nozzle part. The high speed was not permissible, because the laser has less time to heat layer. In this case, laser power should be big enough to heat, but it could burn and make a big hole. To address this problem movement speed should be slow enough to heat layer with half power of laser diode. The bed temperature off our printer is lower compared to traditional and it is lower compared to the recommended value for PLA printing. This is the maximum temperature of the bed that was available.

4.2 Laser control logic

The logic of laser power control is illustrated in **figure 26**.

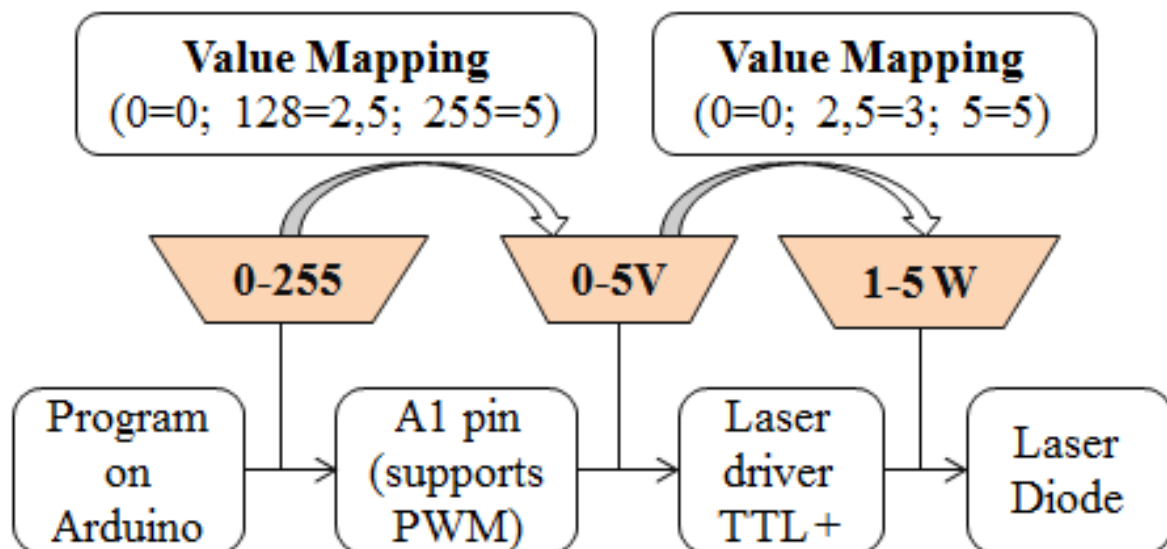


Fig.26. Laser power control logic

Controlling of laser power begins from the program on Arduino, it sends an analog signal to A1 port in the range of 0-255. Then this pins makes value mapping inside, converts the input signal to analog output in the range of 0-5V. This voltage signal further reaches Laser TTL. Inside of the laser pin, it again converts and makes mapping from 1 to 5W. Finally, the laser output voltage corresponds to this value.

4.3 Five Nozzle FDM printer

The laser-assisted FDM process is performed on the 5-nozzle printer. The fabrication process of this printer similar to a conventional extrusion-based printer, except some modifications on mechanism and construction. Schematic view of modern Fused Deposition Modeling based printer shown in **figure 27**. The general printing process begins from the “STL” model format of an object that was drawn on special software. The second step is a special program that is different depending on the printer type. 5-Nozzle printer work is based on “Repetier Host” software. This program makes the slicing process of the STL model. On the user menu, it is possible to adjust printing parameters, for example, printing speed, infill rate, perimeter width, number of external layers and so on. Software is capable of working with multi-extrusion printers. It is possible to choose a different type of extruder for a certain object type. On the setting menu, the user can define nozzle number for a certain 3D object, where could be added color of filament material.

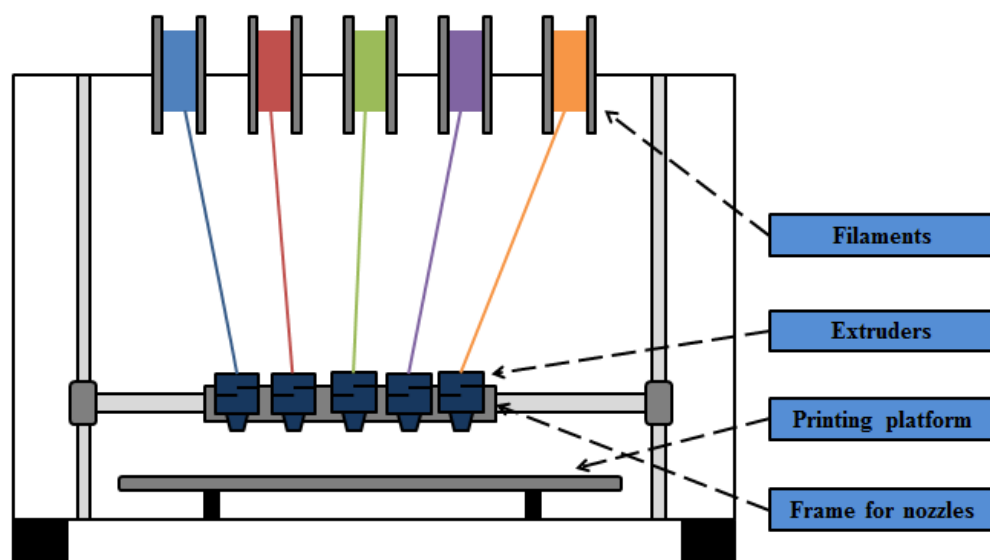


Fig.27. Schematic view of 5-nozzle printer

The FDM fabrication process begins from feeding extruder with the filament. The feed rate of each defined in the program. After reaching filament to the extruder, it is started to

melt. For each filament, there exist recommended printing temperatures. In our experiment, used PLA material, for its extrusion 210C was adjusted. The next step is platform heating; it is necessary for bonding of the first layer of the model to the platform. Movement of the extruder is accomplished by motors that move nozzle part on “x,y” and “z” direction. The main difference of 5 nozzle printer from conventional FDM technology is a number of extruders and their movement mechanism. The schematic drawing of 5 nozzle systems is shown in **figure 28**.

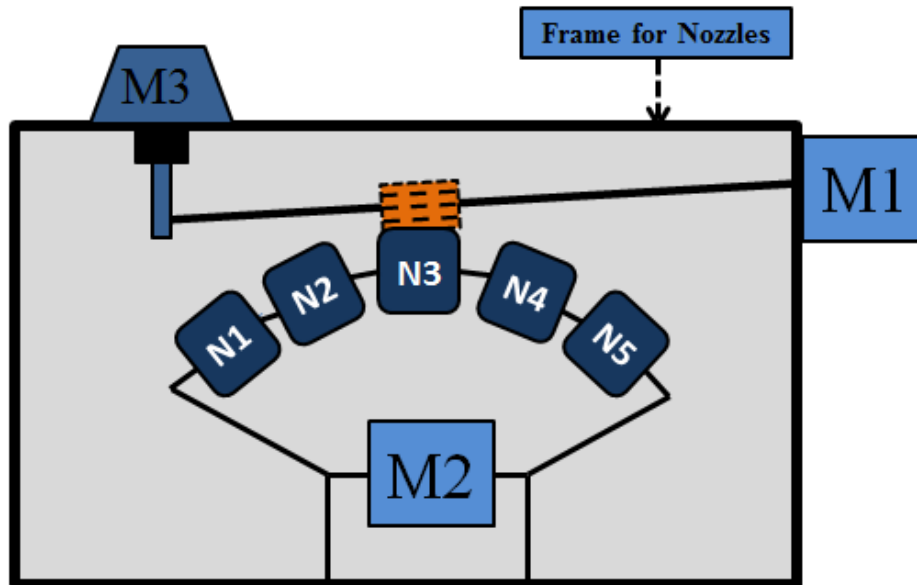


Fig.28. Extruder regulation section of the 5-nozzle printer

The system contains 5 nozzles which are enumerated as “N1, N2, N3, N4, N5”. The motor “M2” is used for rotation of nozzles. “M1” motor used as a feed rate that supplies extruders with the filament. Initially, all filaments are pushed in nozzles. “M3” motor used to push and pull filament feeding roller. The main goal of the system is to change the nozzle and, at the same time, keeps the same reference point of printing. The flow chart below in **figure 29** illustrated the algorithm of the extrusion nozzle switch.

At the first step, M3 motor attaches the roller of motor M1 that feeds extruder with the filament. Further, all nozzles go to the end stopper, and after reading several nozzles, M2 motor rotates the whole system for a certain angle. When the required nozzle settled, M3 motor pushes and roller able to rotate filament. The last step is the M1 motor that performs the filament supply.

Initially, the 5-nozzle printer is gathered by hand and the quality of printed objects was unsatisfactory. Several calibration work and repair was performed. During the multi extrusion process at the moment of the nozzle switch problem was faced. The task was to adjust the

nozzle and change the program code to obtain a precise reference point for each nozzle. Initially, the rotation angle of the nozzle was incorrect because of the deviation in the assembling process. **Figure 30 (a)** shown deviation of nozzle #5 compared to nozzle number #1. A similar problem had other nozzles. To address this problem, the rotation angle was calibrated. Program software gives a certain amount of step number for motor M1. After several corrections of software code successful printing was achieved, which could be seen in **figure 30 (b)**.

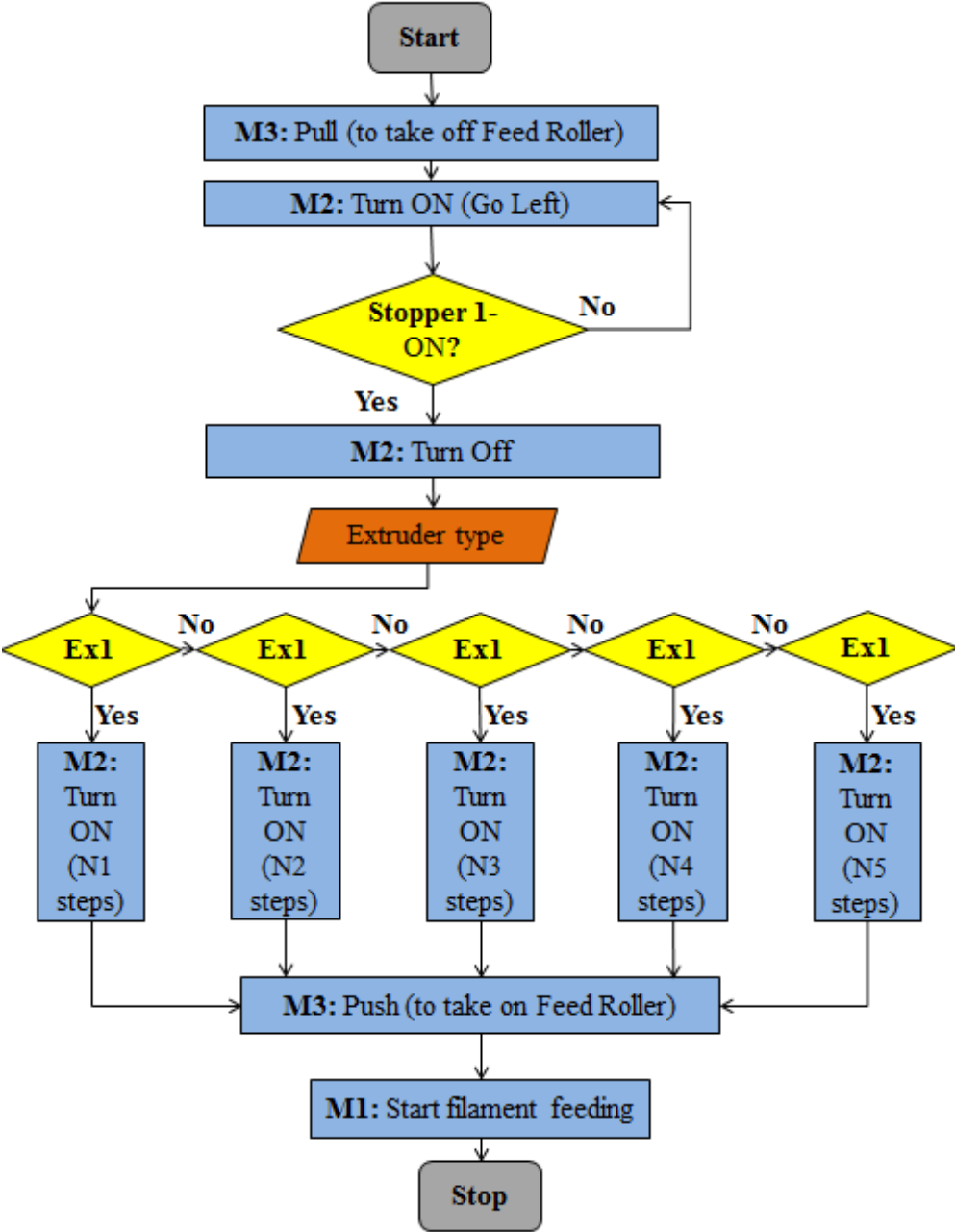


Fig.29. Flow chart of the extrusion switch mechanism

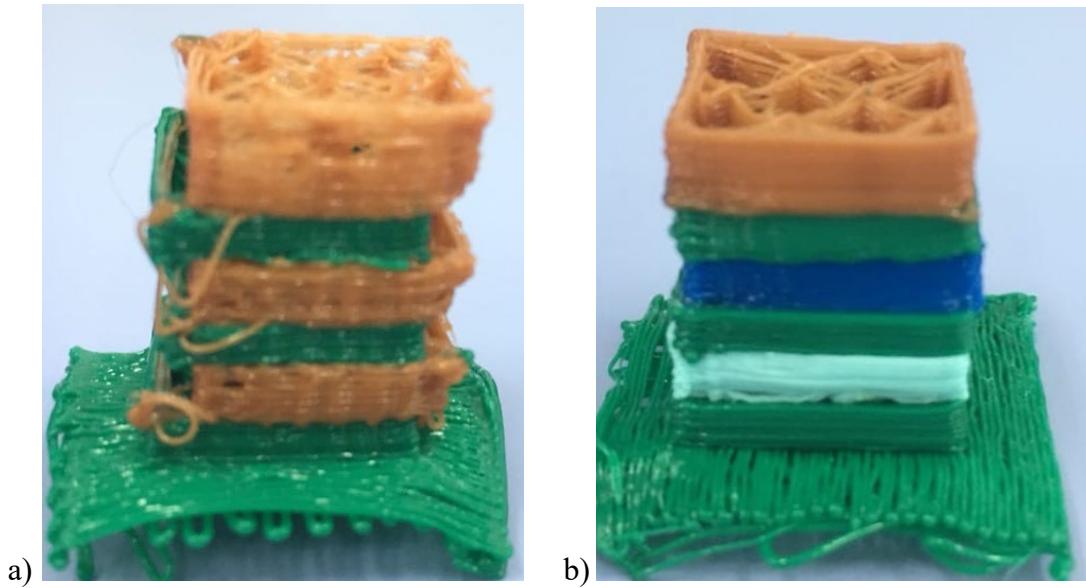


Fig.30. Printing of samples a) before and b) after adjustment

Successful adjustment of reference point was the foundation to print an object that contains up to 5 different material of 5 different colors of one material. The previous specimen was designed especially for adjustment, where only single material extrudes in one layer. On the next stage, it was decided to fabricate a model that could have more than one filament on a single layer. In this case logo of NU was printed several times. The design consisted of 3 colors of PLA material. The base of which printed with green material, the rest top with 2 colors. Overall, the deviation occurred many times. The reason for such behavior was found out. This happened because of the big step size of motor teeth, that rotates nozzles. Even the small-angle causes significant deviation on the other side of the block.



Fig.31. “NU”- logo print

At the moment of nozzle switch, all nozzle change position to the left side and then rotates to the necessary nozzle. The problem occurred during printing; at the moment of sharp turn of extrusion path the motor and frame that holds nozzle shift its position. Although after the change of nozzle reference point is perfect, vibration leads to a change of extrusion position that leads to deviation. The small shift of the figure could be observed in **figure 31** on “brown” color letters. This problem solved by fastening the frame firmly and replacing of stepper motor with another than has for the number of teeth and high precision of rotation.

CHAPTER 5 –EFFECTS OF DESIGN

5.1 Effect of laser on Ultimate tensile strength

Implementation of the new design for enhancing interlayer bonding will bring several improvements relating to the mechanical property of printed object and device installation process. Data analysis based on sample results. It is taken 6 different values of laser power. Laser power values are taken according to PWM signals. It begins at 70 with a step of 15. Corresponding laser value for PWM70- is 1.47 W. For each laser power 5 samples out of 6 were chosen. One sample was eliminated to decrease the standard deviation value. The results of the Ultimate tensile test on the Tinius Olsen machine are listed in *table 6* below. On the table is written laser power for each PWM signal value. Additional samples were taken during the experiment without laser implementation. *Table 5* is a list of cross-sectional dimensions of the sample at the breakpoint.

Table 5. The actual cross-sectional dimensions

Sample # (mm)	Laser Power (PWM value)						
	No Laser	PWM=70 1,47W	PWM=85 1,66W	PWM=100 1,96W	PWM=115 2,25W	PWM=130 2,55W	PWM=145 2,84W
#1	10	9,5	9,1	11	8,5	11,5	9,5
#2	10,5	8,5	10	9	9,5	9	10
#3	9,1	9	9,2	11,5	10	8	11
#4	8,6	9,6	9,2	10,8	9,1	8,5	9,9
#5	8,7	9,5	9,3	11,3	9,4	9,1	10,6

Table 6. Tensile test results

Sample # (MPa)	Laser Power (PWM value)						
	No Laser	PWM=70 1.47W	PWM=85 1.66W	PWM=100 1.96W	PWM=115 2.25W	PWM=130 2.55W	PWM=145 2.84W
#1	16.25	16.12	17.42	18.21	16.65	17.23	17.75
#2	16.13	15.21	17.21	17.22	16.88	17.65	17.68
#3	15.95	15.65	16.81	17.65	15.98	17.04	17.47
#4	16.41	15.88	16.47	17.22	16.32	17.85	17.93
#5	16.33	14.84	16.25	18.21	16.85	16.96	18.08

Figure 32 shows a graphical illustration of the Ultimate tensile test versus Laser power.

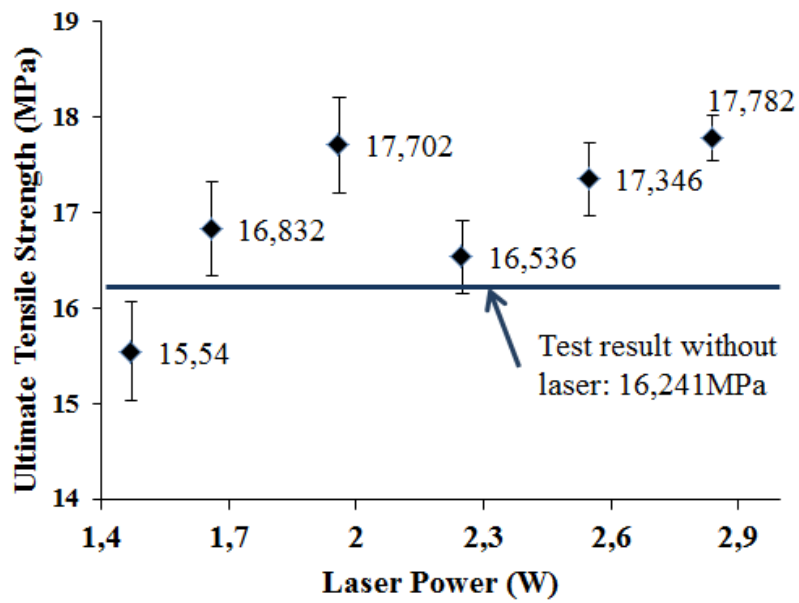


Fig.32. Ultimate stress vs Laser power graph

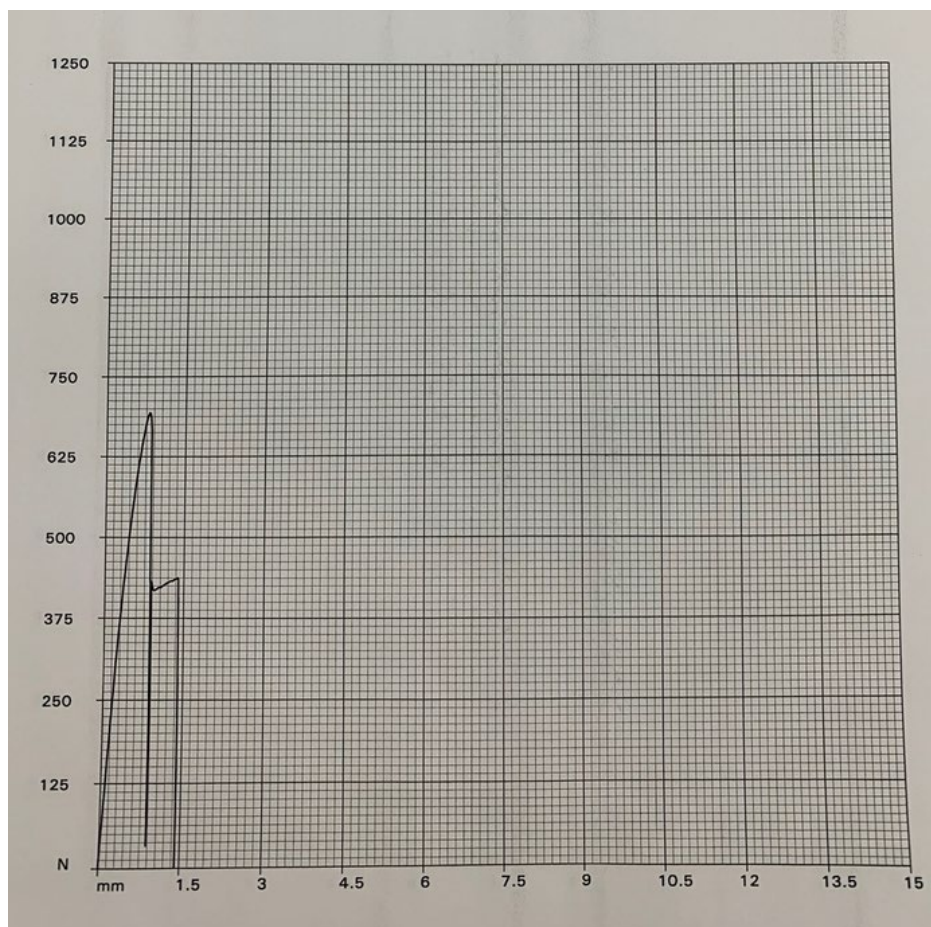


Fig.33. Tensile test results of specimen 3.1 (PWM=100, 1.96W)

Figure 33 illustrated a graphical representation of the tensile test of specimen 3.1, which was fabricated under heating of laser at 1.96Watt. The Tinius Olsen machine represents the displacement of the specimen according to the applied force. To calculate Ultimate tensile strength, it is taken maximum applied force, which is equal to 695N.

$$A = l \times w = 9.54\text{mm} \times 4\text{mm} = 36\text{mm}^2 \quad (1)$$

$$P = \frac{F}{A} = \frac{695\text{N}}{36\text{mm}^2} = 18.21\text{MPa} \quad (2)$$

On formula (1) shown total area formula, where “l”-is the length and “w”-is the width of the specimen part, where the break occurs.

The second formula (2) represented Pressure required to break the specimen, where the letter “F” is employed Force, “A”-is the area, which is calculated with the previous formula.

The horizontal line (blue) on the graph applies to tensile test results without laser assistance. For each laser power values drawn vertical lines, that shows standard deviation. The lowest laser power of 1.47W showed less value of tensile. From the second point, when laser power increased from 1.67W it has a positive impact on laser heating. The highest tensile strength obtained at 1.96W and 2.84W, which corresponds to 17.702MPa and 17.782MPa respectively. The strength of the sample without the laser was 16.241Mpa. Implementation of laser heating increased ultimate tensile strength at maximum point by 9.67% at 2.84W. However, it is suggested to use the laser at 1.96W, because it contributed less energy and shows almost the same enhance, 9%.

The significant range of vertical lines (standard deviation) indicated errors during the experiment, but it is attributed to a change of ambient temperature and unstable extraction and bed temperature. However, it is considered as negligible for experiment results. Another important aspect of the experiment is the color of filament. The color of PLA materials plays a vital role during the healing process. For example, at the beginning of the experiment, the “blue” color PLA was heated. Then it is changed to “brown” color. After, initial heating energy for both colors was chosen. It was concluded that the dark blue color required less laser power for melting, whereas brighter brown color required more energy usage. It is explained with the penetration property of the laser. In the case of a dark color, it has a high penetration coefficient. Consequently, it is important to conduct an experiment with a single material color. In the case of another color, the experiment results could be different, nevertheless positive of laser heating remain the same.

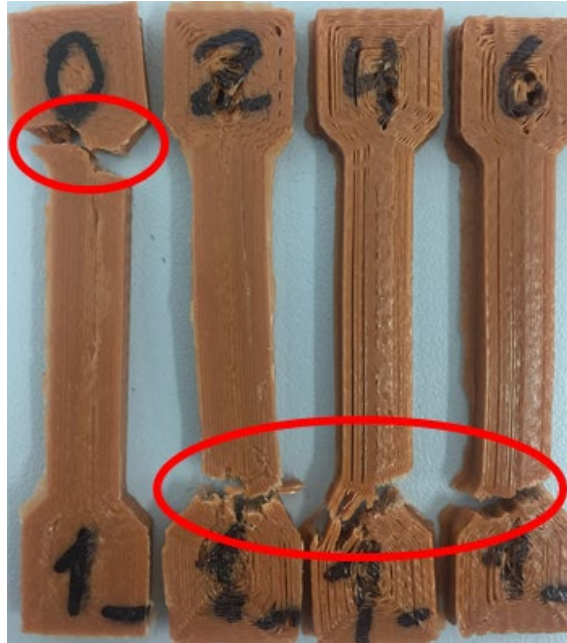


Fig.34. Break point of the specimen

Figure 34 is shown an unusual breakpoint on the specimen during such an experiment. For traditional cases the breaking point after the tensile test lies in the middle of the specimen, which corresponds to the gauge part section. To eliminate all possible errors during measurement of tensile test the experiment was performed under accurate control

The grips were centralized; therefore the proper stress distribution among specimens was achieved. Although the method for precaution was performed, the specimen broke at the shoulder part. There exists different explanation of such behavior of specimen. The first reason is lower bonding at transition region, which is the location between grip and gauge sections. The second reason is the general condition of the FDM printer, which has unsatisfactory printing characteristics. However, as the experiment is done under the same condition, it does not affect general results. The next important aspect of the experiment is printing speed. In the experiment of Ravi *et al.* [38], it is shown that even at the same laser power of 0.75W the Flexural strength changed according to printing speed. The similar pattern observed in the experiment of V. Kishore *et al* [34], where fracture energy differs at different nozzle speeds. Therefore, printing speed should be kept stable. Tensile strength will be changed as printing speed increases.

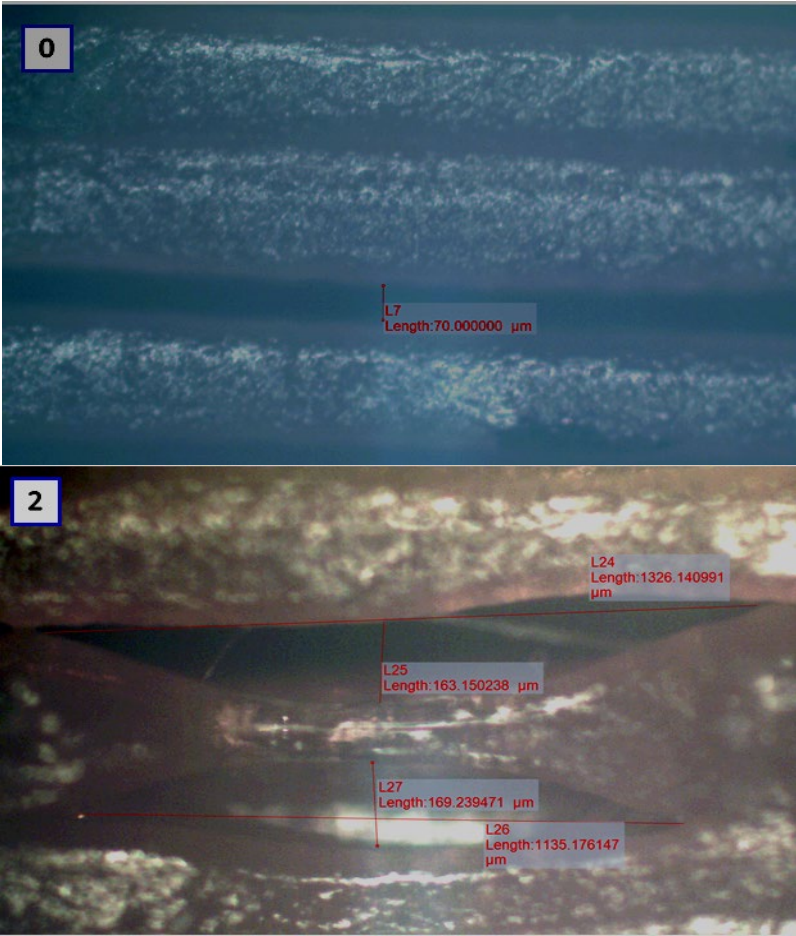
5.2 Effect of laser on surface roughness

The printing samples undergo heating action; therefore, the surface of the printed model differs from the traditional sample. The quality of surface roughness directly depends

on laser power. **Figure 35** is shown the photo of the surface of the specimen. The excess laser power destroys the surface. The sample#0 is printed without laser implementation. The sample#1 printed under the assistance of laser at 1.47W. The last sample#4 is heated with 2.25W laser power. The gradual rise of laser power effects to the more frequent formation of holes and cracks on the surface. A similar negative effect of laser heating was written in the paper of Ravi and his colleagues. [38]



Fig.35. The surface roughness of specimen



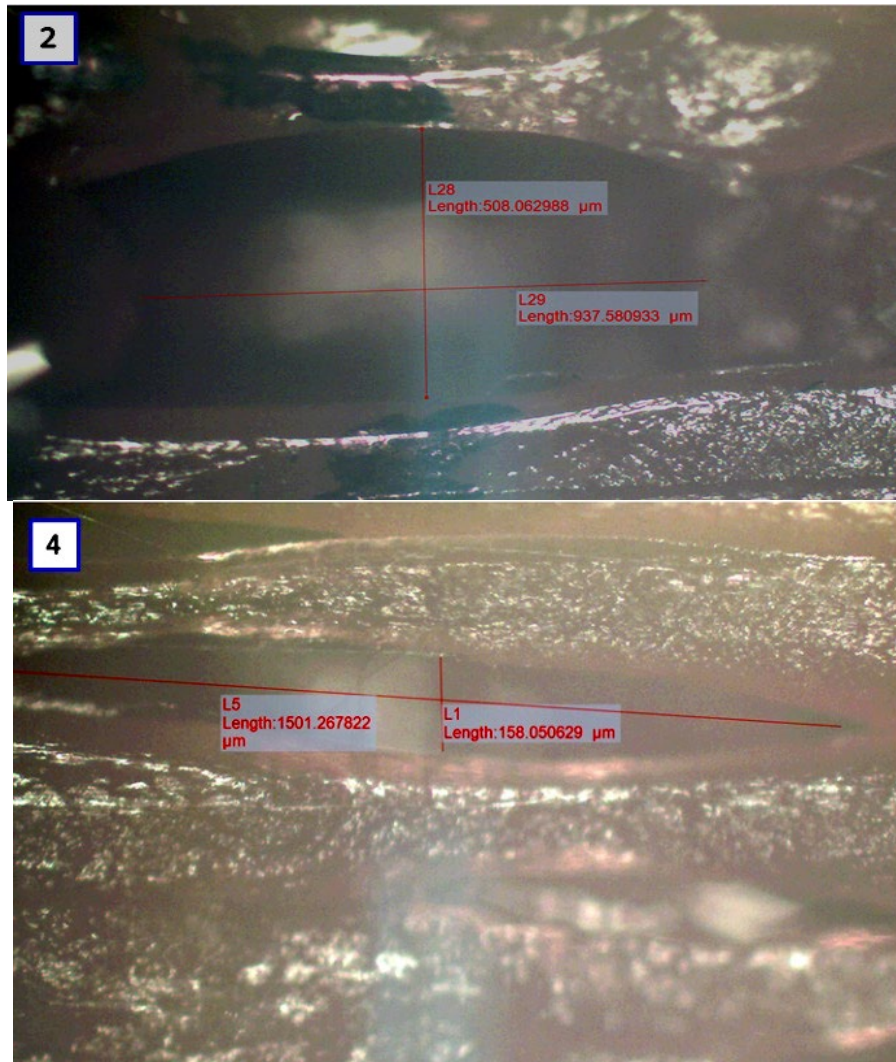


Fig.36. The break formation during laser heating, “#0” without, “#2,4” with laser assistance

The photos of the surface taken by the AE2000-Met apparatus under 50x zoom are shown in **figure 36**. The distance between the neighboring layer on sample#0 is very tiny and this corresponds to without laser printing. The rest of the figures indicate that laser assistance increases the gap between layers of even tear it. For example, on sample #0, the distance is equal to 70μm, whereas on sample #2 is equal to 508 μm.

5.3 Effect of laser implementation on energy consumption

Although the implementation of laser diode enhances interlayer bonding and general mechanical property of a printed object, it requires additional resources.

The key elements of design that differs from traditional FDM printers are diode laser, Arduino controller. To calculate total energy consumption should be used in formula (3).

$$E=Pt \tag{3}$$

$$P = IV = \frac{V^2}{R} = RI^2 \quad (4)$$

The total energy is derived from total power (P) consumption of devices multiplied by total utilization time (t). Formula 4 is shown three different ways of finding total power consumption.

The first step is the calculation of the power consumption of the Arduino Uno controller. The operating voltage of the controller is 5V. The source of energy was the laptop, by which it was connected through USB cable. The clock speed was 16MHz at which wake current is equal to 14mA. The power equation and calculation are written on formula 5.

$$P_c = IV = 14mA * 5V = 0.07W \quad (5)$$

The second step is the calculation of the power consumed by Laser Diode. The working voltage of the laser diode is 12V. Although it is powered by 220V, it has an adapter that converts input DC voltage. The working current of the laser is 5A. The total power generated by the laser diode is calculated in formula 6.

$$P_l = IV = 5A * 12V = 60W \quad (6)$$

The formula of total power consumption is the sum of both devices, laser, and controller, which is calculated in equation 7.

$$P_t = P_c + P_l = 0.07W + 60W = 60.07W \quad (7)$$

To calculate the total energy of the new method, the total power must be multiplied to total operating time. **Figure 37** illustrates the statistical parameters of object printing after slicing on CuraEngine. Tensile test specimen has 20 layers and total printing time equal to 22min 16sec. The total time in seconds is -1336 seconds. It is important to remember that laser was applied after the first layer until the last layer. Hence, the total heated layer number is 18. Consequently, the laser was switch on during 90% of the total time, which is equal to 1202 seconds.

Статистика печати	
Расчетное время:	22 мин:16 с
Слоев:	20
Всего строк:	4877
Длина прутка:	1296 мм
Экструдер 1	1296 мм

Fig.37. Printing time, number of layers and length of filament

The total energy consumption by the new design is calculated on formula 8 and 9.

$$E = P_t t = 60.07W * 1202seconds = 72204,14 J = 72.2kJ \quad (8)$$

$$E = P_t t = 0.06007 kW * 0.3339h = 0.02kWh \quad (9)$$

According to calculation, the implementation of the new method will cost an extra 72.2KJ or 0.02kW*h of energy for printing tensile specimens.

To compare the energy consumption of a 3D printer, it was decided to choose another printer as the printer on which the experiment was carried out is industrial of having a workspace of 1X1m. The moving parts also require more energy compared to conventional FDM printers. Hence, to calculate extra energy value added by the new design, Ender 3 FDM printer was chosen. At average printing speed and platform temperature of 70C during the printing of PLA filament, which has extruder temperature 200-215C it consumes 0.125kWh energy for 1 hour.

Let us calculate the consumption of energy by laser and controller for 1 hour.

$$E = P_t t = 60.07W * 3600seconds = 216252 J = 216,252 kJ \quad (10)$$

$$E = P_t t = 0.06007 kW * 1 h = 0.06kWh \quad (11)$$

From the results of equation 11, it is calculated that 1-hour usage of laser+controller is equal to 0.06kWh. Further assessment is related to the total energy rate increase of new design, compared to traditional FDM. On equation 12 shown the formula, where

$$Increase\ Rate = \frac{E_{nd}}{E_T} = \frac{E_T + E_L}{E_T} = \frac{0.125kWh + 0.06kWh}{0.125kWh} * 100\% = 148\% \quad (12)$$

E_T -is energy by the traditional method

E_L -energy by laser implementation

E_{nd} -new design energy

It is calculated that the implementation of the diode laser and Arduino controller increases total energy consumption to 148%.

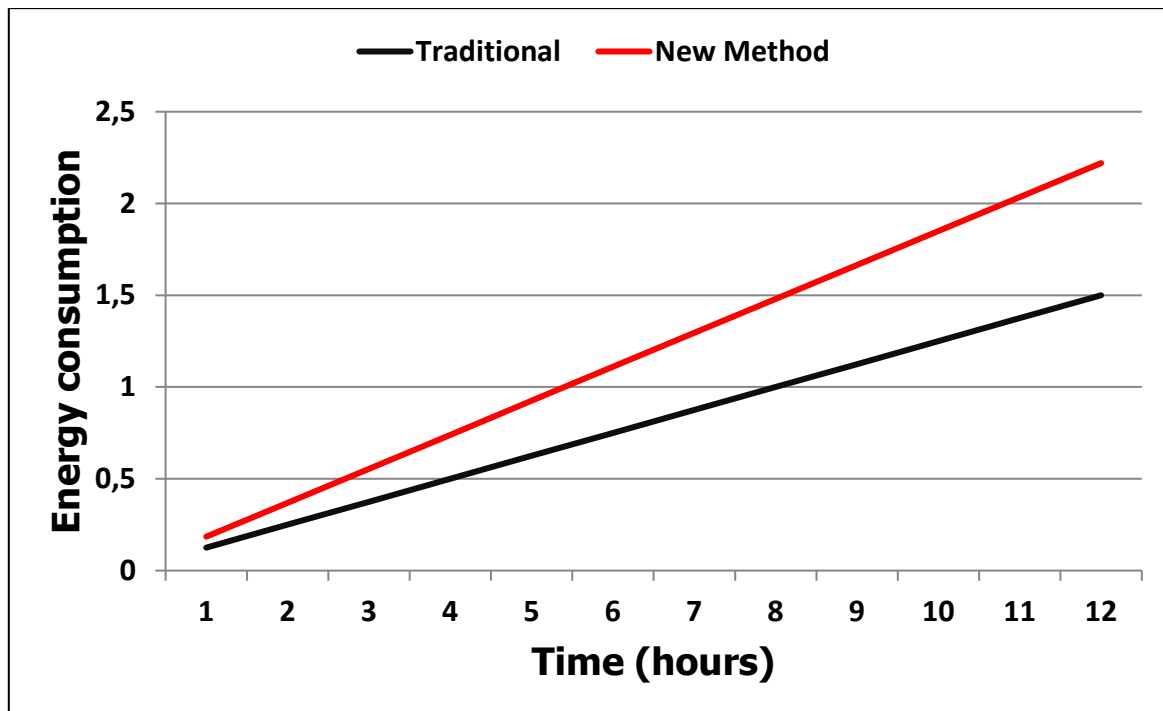


Fig.38. Energy consumption of traditional and new method

To illustrate the effect of implementing new devices the graphical representation of energy consumption is shown in **figure 38**. It is obvious that additional energy load will influence more and more as the printing time increases.

5.4 Effect of laser implementation on the economic value

Assessment of the economic part is very important to understand the influence of the development of the FDM system via Laser-assisted heating. The previous part illustrates the negative impact of improvement on energy consumption. This paragraph intended to calculate additional expenses, including device purchase and electricity bin.

Table 7 listed all the necessary information required to calculate the economic effect of the new design. First of all, it includes the price of Laser Diode that was purchased from AliExpress. The second component is the Arduino Uno controller, which comes from laboratory storage. The third component is the market price of the Ender 3 FDM printer. The reason for such choice is the previous calculation during energy consumption. To make a comparison with the traditional FDM printer, this model was chosen. Another important parameter is a dollar to tenge course. It was chosen $380\text{T}=1\text{\$}$. The last element is the price of electricity for 1kWh of energy. The price of electricity taken the latest tariff of Almaty city, by LLP “АлматыЭнергоСбыт” manufacturer.

Table 7. Economical table value with price

Component	Price in Tenge (380T=1\$)	Price in \$
Diode laser 450nm, 5W	41256	108.56
Arduino Uno Rev3	12750	-
Ender 3 Pro	100700	265
1kWh energy	19.17	-

The total price of the new FDM machine is written in formula 13.

$$P_t = P_{\text{ender}} + P_{\text{laser}} + P_{\text{controller}} = 41256 + 12750 + 100700 = 154,706 \text{ tenge} \quad (13)$$

The calculation of the increase rate of hardware price of the new design is shown in formula 14 below.

$$\text{Increase Rate} = \frac{P_{nd}}{P_T} = \frac{P_T + P_L}{P_T} = \frac{100700 + 41256 + 12750}{100700} * 100\% = 153\% \quad (14)$$

P_T -price of the traditional method

P_L - the price of laser implementation

P_{nd} -new design price

The fixed price of the new design that includes laser and controller is 154.706 t, compared to the traditional Ender PRO 3 value it is increased by 153%. However, there did not take into account the electricity consumption price.

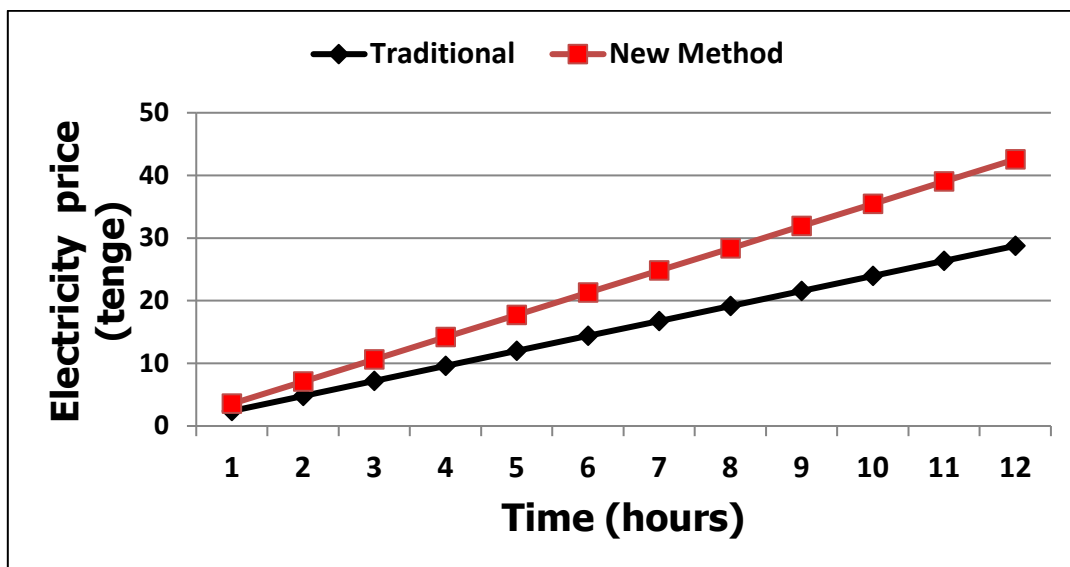


Fig.39. Expenses for electricity of traditional and new method

Figure 39 shown the line graph which represents how much money spent during the utilization of the traditional FDM printer (Ender 3) and laser improved new design. In the case of printing some models for a few hours, the difference between the expenses does not become significant. However, for a long period, the influence of energy consumption will be more considerable. For example, let's assume that the average usage of the printer for 1 week will be 36 hours (6 hours per day, 6 days a week).

$$PY_{nd} = 36 \text{ hours/week} * 52 \text{ week} * 19.17 \text{ kWh/tenge} * 0.185 \text{ kWh} = 6639 \text{ tenge} \quad (15)$$

$$PY_t = 36 \text{ hours/week} * 52 \text{ week} * 19.17 \text{ kWh/tenge} * 0.125 \text{ kWh} = 4486 \text{ tenge} \quad (16)$$

On formulas 15 and 16 is shown total expenses for electricity for 1 year with new and old methods. For traditional purpose user pays 4486 tenges, whereas, for the new method, the user will pay 6639 tenges; these calculations based on the same operating time.

CHAPTER 6-CONCLUSION & FUTURE

WORK

6.1 Conclusion

The innovative design of heat treatment during the FDM process is demonstrated in this paper. Interlayer bonding enhanced during diode laser-assisted heating, which has a 452nm wavelength. The ultimate tensile test showed a 9.67% increase at 2.84W power of the laser. At different values of laser power, tensile strength showed dissimilar tendency. For example, if at the lower value it was below compared to the traditional method and increased until 17.702, then it decreased suddenly at 1.96W. Afterward, it again illustrated the rising curve. That kind of result could indicate a discrepancy with direct linear dependences with laser power. Nevertheless, that kind of fluctuation could be the indicator of the effect of other aspects of the experiment as an ambient condition.

However, the implementation of the diode laser had a negative consequence on the surface roughness of printed objects. The image taken by the AE2000-met device showed that excessive heating of the laser damages surface of the specimen. The experiment covered under certain printing speed and used brown color of PLA material, and it is important to note, that these figures correspond to a certain condition. Different printing speed and filament color will show different values. The new technology of laser-assisted heating systems could be implemented for most of the types of 3D printers. Direct attachment of laser diode on the nozzle part makes it is suitable for implementation. Compared to other technologies, where is no need for additional components as mirrors. Another benefit of this method is a simple control technology. It is pretty easy to write logic on the Arduino platform and adjust laser power via its controller. This work is given a full explanation of the control system. It has very good potential because, during printing with different filaments, it could be regulated for certain power for specific printing material.

The tensile test result graph indicates a significant value of standard deviation. This problem is attributed to the change of some parameters during printing the sample at a certain value. The main reason is the extruder temperature. At the printing temperature of 210, it showed fluctuation between 208-213. Another impact is bed temperature, at a settled temperature of 52, it slowly falls to 50C and even 49C. The last temperature parameter is the

condition of the laboratory. The experiment covered for 2-3 weeks, the average temperature of the room is 20C. Another aspect of the experiment is the actual size of the specimen. Even at the same value of thickness, the length and width were slightly different, however, it is a normal situation of samples printed by the FDM printer. All these values in combination could affect the deviation of results.

The effect of laser implementation and new design on electricity consumption and financial aspect was analyzed. According to calculation, the required energy value increased to 48%, which means that if a user prints an object for 1 hour, the total spending of energy rises almost half times. However, such frightening numbers are not so terrifying, because even the implementation of laser and controller will take 0.185kWh, which is very low. Further calculations performed based on the extra money expenses of the user. The fixed price of all required equipment increased by 53%, from 100,700 tenges to 154,700 tenges. Although the energy rate increased, the money spends on electricity not significant. The total assumed expenses for one year and the difference between the new and old method is only 2153 tenge. That kind of calculation brings to the idea that a 9.67% increase in tensile strength for the user will cost cheaply for electricity, but the initial fixed cost for purchasing apparatus “tangible”.

6.2 Future work

Further research on this topic will be concentrated on the multi-directional heating process, where could be used 3 diode laser. However, before this experiment, the current design should be optimized to decrease the significant deviation of the Ultimate tensile strength value. The control concept and design for this are described in this paper. Another research area is print with different filaments as ABS and PEEK. After identifying perfect laser power for each filament, multi-material printing could be tested. It was explained that printing speed has a considerable impact on test results, therefore the different values of nozzle speed correspond to different laser power values, that heats the filament to the glass transition temperature. Furthermore, investigate the effect of pre-deposition heating on flexural strength, bending and shear strength also an attractive topic. The last research area will be calculating and analyzing the impact of laser employment on the environment by performing Life cycle assessment.

REFERENCES

- [1] Siqueiros, H. I. M. Castillo and J. Z., "Design and Manufacturing Strategies for Fused Deposition Modelling in Additive Manufacturing : A Review," *Chinese J. Mech. Eng.*, 2019.
- [2] Jianbin, S et al., "Comparison of Different Types of 3D Printing Technologies," vol. 8, pp. 1-9, 2018.
- [3] D. Depuydt et al., "Production and Characterization of Bamboo and Flax Fiber Reinforced Polylactic Acid Filaments for Fused Deposition Modeling (FDM)," *Polymer composites*, 2018.
- [4] A. Awad et al, "Fused Deposition Modelling : Advances in Engineering and Medicine," *3D Printing of Pharmaceuticals*, p. 107–132.
- [5] Yu-an Jin et al., "Optimization of tool-path generation for material extrusion-based additivemanufacturing technology," 2014.
- [6] Md. Hazrat Ali et al., "Material Optimization Method in 3D Printing," *IEEE International Conference on Advanced Manufacturing*, pp. 365-368, 2018.
- [7] Pavan K. Gurrala et al., "Part strength evolution with bonding between filaments in fused deposition modelling," *Virtual and Physical Prototyping*, July,2014.
- [8] T.Jerome et al., "Bond and part strength in fused deposition modeling," *Rapid Prototyping Journal*, vol. 23, p. 2, 2017.
- [9] Vishwas, C. K. Basavaraj and M., "Studies on Effect of Fused Deposition Modelling Process Parameters on Ultimate Tensile Strength and Dimensional Accuracy of Nylon," *IOP Conf. Ser.: Mater. Sci. Eng.*, 2016.
- [10] Hongbin Li et al., "The effect of process parameters in fused deposition modelling on bonding degree and mechanical properties," *Rapid Prototyping Journal*, December,2017.
- [11] Ngoc-Hien Tran et al., "Study on the Effect of Fused Deposition Modeling (FDM) Process Parameters on the Printed Part Quality," *Journal of Engineering Research and Application*, vol. 7, pp. 71-77, December 2017.
- [12] K.G. Jaya Christiyana et al., "A study on the influence of process parameters on the Mechanical Properties of 3D printed ABS composite," *IOP Conf. Ser.: Mater. Sci. Eng.*, vol. 114, 2016.
- [13] Hongbin Li et al., "The Quantitative Research of Interaction between Key Parameters

- and the Effects on Mechanical Property in FDM," *Advances in Materials Science and Engineering*, 2017.
- [14] Filip Górski et al., "Influence of process parameters on dimensional accuracy of parts manufactured using FDM technology," *Advances in Science and Technology*, vol. 7, pp. 27-35, Sept.2013.
- [15] Aboma W. G et al., "Investigating Effects of Fused-Deposition Modeling (FDM) Processing Parameters on Flexural Properties of ULTEM 9085 using Designed Experiment," *Materials*, pp. 1-23, 2018.
- [16] Petr Vosynek et al., "Influence of Process Parameters of Printing on Mechanical Properties of Plastic Parts Produced by FDM 3D Printing Technology," *MATEC Web of Conferences*, 2018.
- [17] D. C. Rajan Narang, "Analysis of Process Parameters of Fused Deposition Modeling (FDM) Technique," *International Journal on Future Revolution in Computer Science & Communication Engineering*, vol. 3, Oct,2017.
- [18] Lu Wang et al., "Effect of fused deposition modeling process parameters on the mechanical properties of a filled polypropylene," *Progress in Additive Manufacturing*, 2018.
- [19] Omar Ahmed Mohamed et al., "Effect of Process Parameters on Dynamic Mechanical Performance of FDM PC/ABS Printed Parts Through Design of Experiment," *Journal of Materials Engineering and Performance*, 2016.
- [20] D. Popescu et al., "FDM process parameters influence over the mechanical properties of polymer specimens: A review," *Polymer Testing*, 2018.
- [21] Yongnian Yan et al., "Research on the bonding of material paths in melted extrusion modeling," *Materials & Design*, pp. 93-99, 2000.
- [22] Martin Spoerk et al., "Effect of the printing bed temperature on the adhesion of parts produced by fused filament fabrication," *Plastics, Rubber and Composites*, 2017.
- [23] Claire Benwood et al., "Improving the Impact Strength and Heat Resistance of 3D Printed Models: Structure, Property, and Processing Correlationships during Fused Deposition Modeling (FDM) of Poly(Lactic Acid)," *ACS Omega*, vol. 3, p. 4400–4411, 2018.
- [24] S. Naghieh, M.R. Karamooz Ravar et al., "Numerical investigation of the mechanical properties of the additive manufactured bone scaffolds fabricated by FDM: the effect of

- layer penetration and post-heating," *Journal of Mechanical Behavior of Biomedical Materials*, pp. 1-21, 2016.
- [25] Emily R. Fitzharris et al., "Interlayer bonding improvement of material extrusion parts with polyphenylene sulfide using the Taguchi method," *Additive Manufacturing*, 2018.
- [26] Wonjin Jo et al., "Investigation of influence of heat treatment on mechanical strength of FDM printed 3D objects," *Rapid Prototyping Journal*, 2018.
- [27] Amir Reza Zekavat et al., "Investigating the effect of fabrication temperature on mechanical properties of fused deposition modeling parts using X-ray computed tomography," *Int J Adv Manuf Technol*, 2018.
- [28] Chuncheng Yang et al., "Influence of thermal processing conditions in 3D printing on the crystallinity and mechanical properties of PEEK material," *Journal of Materials Processing Tech*, vol. 248, pp. 1-7, 2017.
- [29] Vladimir E. Kuznetsov et al., "Increasing of strength of FDM (FFF) 3D printed parts by influencing on temperature-related parameters of the process," pp. 1-32, 2018.
- [30] Michael Arthur Cuiffo et al., "Impact of the Fused Deposition (FDM) Printing Process on Polylactic Acid (PLA) Chemistry and Structure," *MDPI*, pp. 1-14, 2017.
- [31] Q. Sun et al., "Effect of processing conditions on the bonding quality of FDM polymer filaments," *Rapid Prototyping Journal*, vol. 14, pp. 72-80, 2008.
- [32] S. Maidin et al., "Effect of Vacuum Assisted Fused Deposition Modeling on 3D Printed ABS Microstructure," *International Journal of Applied Engineering Research*, vol. 12, pp. 4877-4881, 2017.
- [33] Jun Yin et al., "Interfacial bonding during multi-material fused deposition modeling (FDM) process due to inter-molecular diffusion," *Materials Design*, vol. 150, pp. 104-112, 2018.
- [34] Vidya Kishorea et al., "Infrared preheating to improve interlayer strength of big area additive manufacturing (BAAM) components," *Additive Manufacturing*, vol. 14, pp. 7-12, 2017.
- [35] S. C. Partain, "FDM with localized pre-deposition heating using forced air," *Master's Thesis, Montana State University*, 2007.
- [36] Meng Luo et al., "Controllable interlayer shear strength and crystallinity of PEEK components by laser-assisted material extrusion," *Materials Research Society*, vol. 33,

pp. 1632-1641, 2018.

- [37] Du Jun et al., "An improved fused deposition modeling process for forming large-size thin-walled parts," *Journal of Materials Processing Technology*, vol. 234, pp. 332-341, 2016.
- [38] Abinesh Kurapatti Ravi et al., "An in-process laser localized pre-deposition heating approach to inter-layer bond strengthening in extrusion based polymer additive manufacturing," *Journal of Manufacturing Processes*, vol. 24, p. 179–185, 2016.
- [39] Berke Ricketti, "Diode Laser Characteristics," 2015.
- [40] G. P. Agrawal, and N. K. Dutta, "Infrared and Visible Semiconductor Lasers," *Semiconductor Lasers*, pp. 547-582, 1993.
- [41] Y. Arakawa, and H. Sakaki, "Multidimensional quantum well laser and temperature dependence of its threshold current," *Applied Physics Letters*, vol. 40, pp. 939-941, 1982.

APPENDIX A: Publication

[1] Nurbol Sabyrov, Anuar Abilgazyev, and Md. Hazrat Ali, “Enhancing Interlayer Bonding Strength of FDM 3D Printing Technology by Diode Laser-Assisted System,” *The International Journal of Advanced Manufacturing Technology*.(2020). Accepted with correction. Springer, Q1, Impact factor: 2.496.

[2] Nurbol Sabyrov, Anuar Abilgazyev, Zhuldyz Sotsial, and Md. Hazrat Ali “Design of a flexible neck orthosis on FDM printer for rehabilitation and daily usage,” *10th CIRP Sponsored Conference on Digital Enterprise Technologies (DET 2020) – Digital Technologies as Enablers of Industrial Competitiveness and Sustainability*. Proceedia Elsevier, Submitted.